



PAPER

Quantum criticality in a Kondo quantum dot coupled to helical edge states of interacting 2D topological insulators

Chung-Hou Chung^{1,2} and Salman Silotri¹¹ Department of Electrophysics, National Chiao-Tung University, HsinChu, Taiwan, 300, Republic of China² National Center for Theoretical Sciences, HsinChu, Taiwan 300, Republic of China

E-mail: chung@mail.nctu.edu.tw

Keywords: Kondo effect, quantum criticality, quantum dot, topological insulators

RECEIVED

9 October 2014

ACCEPTED FOR PUBLICATION

24 November 2014

PUBLISHED

9 January 2015

Content from this work
may be used under the
terms of the [Creative
Commons Attribution 3.0
licence](#).

Any further distribution of
this work must maintain
attribution to the author
(s) and the title of the
work, journal citation and
DOI.



Abstract

We investigate theoretically the quantum phase transition (QPT) between the one-channel Kondo (1CK) and two-channel Kondo (2CK) fixed points in a quantum dot coupled to helical edge states of interacting 2D topological insulators (2DTI) with Luttinger parameter $0 < K < 1$. The model was studied by Law *et al* (2010 *Phys. Rev. B* **81** 041305(R)), and was mapped onto an anisotropic two-channel Kondo model via bosonization. For $K < 1$, the strong coupling 2CK fixed point was argued to be stable for infinitesimally weak tunnelings between the dot and the 2DTI based on a simple scaling dimensional analysis (Law *et al* 2010 *Phys. Rev. B* **81** 041305(R)). We re-examine this model beyond the bare scaling dimension analysis via a one-loop renormalization group (RG) approach combined with bosonization and re-fermionization techniques near weak-coupling and strong-coupling (2CK) fixed points. We find for a fixed value of $K < 1$ that the 2CK fixed point can be unstable towards the 1CK fixed point and the system is expected to undergo a quantum phase transition between 1CK and 2CK fixed points with changing Kondo couplings. Our RG approach is controlled near $K = 1$. In general, this QPT can also occur upon tuning the Luttinger parameter K to a critical value K_c smaller than unity ($0 < K_c < 1$) for fixed Kondo couplings. The QPT in our model comes as a result of the combined Kondo and the helical Luttinger physics in 2DTI, and it serves as the first example of the 1CK-2CK QPT that is accessible by the controlled RG approach. We extract quantum critical and crossover behaviors from various thermodynamical quantities near the transition. Our results are robust against particle-hole asymmetry for $\frac{1}{2} < K < 1$.

1. Introduction

Quantum phase transitions (QPTs) [1], the phase transitions at zero temperature due to competing quantum ground states or quantum fluctuations, in correlated electron systems are of great fundamental importance and have been intensively studied over recent decades. Of particular interest are continuous QPTs where universal scaling behaviors in observables are expected near criticality. Very recently, nanosystems (such as quantum dots [2]) have provided an excellent playground in which to study QPTs due to high tunability [3, 4, 6–11]. The well-known Kondo effect [12, 13] plays a crucial role in understanding low energy properties in quantum dot devices. Potential new QPTs in these systems may be realized in connection to exotic Kondo ground states. An outstanding example of an exotic Kondo state is the two-channel Kondo (2CK) system [14–19], which has attracted much attention as it shows non-Fermi liquid behaviors at low temperatures. Experimentally, the 2CK behaviors have been realized in various quantum impurity systems such as a quantum dot independently coupled to an infinite and a finite reservoir of non-interacting conduction electrons [20], magnetically doped metal junctions [21], and a metal point contact [22].

More interestingly, the 2CK physics has also been found theoretically in a Kondo quantum dot coupled to two strongly interacting Luttinger liquid leads with Luttinger parameter $K < \frac{1}{2}$ (see [23, 25]). In this case, electron-electron interactions in the leads strongly suppress the cross-channel Kondo correlations responsible for charge transport through the quantum dot while the Kondo correlations involving electrons on the same lead are

unaffected, leading to a two-channel Kondo ground state where two independent Kondo screenings occur between the spins on the dot and in each lead separately. However, for weaker electron interactions, $K > \frac{1}{2}$, both kinds of Kondo scattering involving conduction electrons on the same and different leads become relevant at low energies, giving rise to a 1CK ground state where only a single channel of the conduction electrons in the two leads (the even combination of the electrons in the two leads) effectively couples to the Kondo dot. An exotic quantum phase transition at $K = \frac{1}{2}$ between the 1CK phase for $K > \frac{1}{2}$ and the 2CK behaviors for $K < \frac{1}{2}$ is therefore expected [23]. However, the critical properties of this 1CK-2CK QPT have not yet been properly addressed in these systems due to the lack of controlled theoretical approaches near the strong coupling 2CK fixed point (though this issue was recently studied in the Kondo-polaron model [24]).

However, recently a new type of materials—topological insulators (TIs)—with a gapped bulk and gapless edge states has been proposed theoretically [26] and realized experimentally [27]. In 2D TIs, the gapless edge states have a ‘helical’ nature, i.e. the directions of spin and momentum are locked together [28]. Based on bosonization and a simple scaling dimension analysis, the 2CK behaviors were argued to be stabilized in a Kondo quantum dot coupled to two interacting helical edge states of 2D TIs as long as a weak electron-electron interaction exists in the helical electrons ($K < 1$) [29]. However, on a general ground, similar competition between the cross-channel Kondo correlation and suppression of tunneling due to electron-electron interactions mentioned above is also expected here for the helical Luttinger liquid, a special type of Luttinger liquid with broken SU(2) symmetry. The exotic 1CK-2CK QPT is therefore expected to occur in this new setup.

In this paper, we re-examine the system in [29] near a 2CK fixed point to explore the possibility of the exotic 1CK-2CK QPT via the controlled one-loop renormalization group (RG) approach combined with bosonization, which goes beyond the bare scaling dimension analysis in [29]. For a weak but finite lead-dot tunneling, we find that for $K \rightarrow 1^-$ where our RG approach is well controlled the 2CK fixed point can be unstable towards the (anisotropic) 1CK fixed point and the system is expected to undergo a quantum phase transition between 1CK and 2CK fixed points. The QPT in our model comes as a result of the combined Kondo and the helical Luttinger physics in 2DTIs. It serves as the first example of the 1CK-2CK QPT that is accessible by the controlled perturbative RG approach. The stability analysis on these two fixed points shows that they are stable against small particle-hole asymmetry for $\frac{1}{2} < K < 1$. We extract the non-Fermi liquid behaviors from various thermodynamical quantities at the 1CK-2CK quantum critical point.

This paper is organized as follows. In section 2, we introduce the model Hamiltonian and its bosonized form as shown in [29]. In section 3.1 we present the RG analysis of the model in the weak coupling limit via the bosonization approach (see appendix A). In section 3.2 we further map our bosonized model onto an effective Kondo model via re-fermionization near the strong-coupling 2CK fixed point. We then perform the RG analysis via both poor-man’s scaling (see appendix B) and the field-theoretical ϵ -expansion technique (see appendix C). We also check our RG analysis near the strong-coupling 2CK fixed point obtained from re-fermionization via an alternative way based directly on the RG analysis of the bosonized Hamiltonian near the 2CK fixed point (see appendix D). Our RG analysis in both limits predicts a quantum phase transition between 1CK and 2CK fixed points. In section 4 we perform stability analysis on the 1CK and 2CK fixed points. We find that both fixed points are stable for $\frac{1}{2} < K < 1$, which substantiates our main finding that there exists unstable quantum critical points separating two stable 1CK and 2CK fixed points near $K = 1$. In section 5, we calculate via the field-theoretical ϵ -expansion approach the critical properties and crossover functions of various thermodynamic observables. In section 6, we emphasize the clear physical picture of our main findings and draw conclusions.

2. Model Hamiltonian

In our setup, the Kondo Hamiltonian has the same form as in [29], given by

$$\begin{aligned}
 H &= H_0 + H_K + H_{\text{int}}, \\
 H_0 &= -iv_F \sum_{i=1,2} \int_{-\infty}^{\infty} dx \left[c_{i,R}^{\dagger\uparrow}(x) \partial_x c_{i,R}^{\dagger}(x) \right. \\
 &\quad \left. - c_{i,L}^{\dagger\downarrow}(x) \partial_x c_{i,L}^{\dagger}(x) \right], \\
 H_K &= \sum_{i=1,2} J_1 \vec{S} \cdot \vec{s}_{i,i} + \sum_{i \neq j} J_2 \vec{S} \cdot \vec{s}_{i,j}, \\
 H_{\text{int}} &= \sum_{i,\sigma=\uparrow\downarrow} g_4 \int [c_{i,\alpha}^{\dagger\sigma}(x) c_{i,\alpha}^{\sigma}(x)]^2 dx \\
 &\quad + g_2 \int c_{i,R}^{\dagger\uparrow}(x) c_{i,R}^{\dagger}(x) c_{i,L}^{\dagger\downarrow}(x) c_{i,L}^{\dagger}(x) dx.
 \end{aligned} \tag{1}$$

Here, H_0 describes the two conduction electron baths (labeled as lead 1 and lead 2) made of helical edge states in 2D topological insulators, H_K is the Kondo interaction, and the electron-electron interactions with forward scattering $g_{2,4} > 0$ terms are given by H_{int} with $i = 1, 2$ the lead index, and $\alpha = \text{R, L}$ being the label of the right (R) and left (L) moving electrons in the helical edge state. The conduction electron spin operator is given by: $\vec{S}_{i,j} = \sum_{k,k',\gamma,\delta} c_{ki}^{\dagger\gamma} \cdot \frac{\vec{\sigma}_{\gamma\delta}}{2} \cdot c_{k'j}^{\delta}$ with $\gamma, \delta = \uparrow, \downarrow, i, j = 1, 2$. The local impurity spin operator on the quantum dot can be expressed in terms of pseudo-fermion operator f_{σ} [30]: $\vec{S} = \sum_{\gamma,\delta} f_{\gamma}^{\dagger} \cdot \frac{\vec{\sigma}_{\gamma\delta}}{2} \cdot f_{\delta}$. In the Kondo limit of our interest, the impurity (quantum dot) is singly-occupied: $\sum_{\sigma=\uparrow,\downarrow} f_{\sigma}^{\dagger} f_{\sigma} = 1$. Here, the coupling J_1 and J_2 in H_K stand for the strength of the Kondo correlations between the dot and electrons on the same and different leads, respectively. Note that in the presence of spin-orbit coupling, the spins \uparrow/\downarrow of the helical edge state electrons are locked with their right-moving (R)/left-moving (L) momentum. Note also that the small spin-orbit coupling will break the SU(2) spin-rotational symmetry in the above isotropic Kondo model, leading to the anisotropic Kondo model with $J_i^{xy} \neq J_i^z$ (see [29]).

The Hamiltonian equation (1) can be bosonized through the standard Abelian bosonization [31] for the electron operator [29, 32]: $c_{i,\text{R/L}} = \frac{1}{\sqrt{2\pi a}} F_{i,\text{R/L}} e^{\pm i(\sqrt{4\pi}\phi_{\text{R/L}}(x) + k_F x)}$; the bosonic fields $\phi_i(x) = \phi_{i\text{L}}(x) + \phi_{i\text{R}}(x)$, $\theta_i(x) = \phi_{i\text{L}}(x) - \phi_{i\text{R}}(x)$. The dual fields $\phi_i(x)$ and $\theta_i(x)$ obey the commutation relations: $[\phi_i(x), \theta_j(x')] = \frac{-i}{2} \delta_{ij} \text{sgn}(x - x')$ with $\text{sgn}(x = 0) = 0$. The symmetric and antisymmetric combinations of ϕ_i, θ_i are defined as: $\phi_{s/a} = \frac{1}{\sqrt{2}}(\phi_1 \pm \phi_2)$ and $\theta_{s/a} = \frac{1}{\sqrt{2}}(\theta_1 \pm \theta_2)$. Here, $F_{i,\text{R/L}}$ are the Klein factors to preserve the anti-commutation relations between fermions (electrons) in the bosonized form, and a is the lattice constant (lower bound in length scale); we have also dropped the spin indices of the edge state electrons due to their helical nature. The bosonized Hamiltonian after rescaling the boson fields, $\phi_{a,s} \rightarrow \sqrt{\frac{1}{K_{\sigma}}} \phi_{a,s}, \theta_{a,s} \rightarrow \sqrt{\frac{1}{K_{\rho}}} \theta_{a,s}$, is given by [29]:

$$\begin{aligned}
H &= H_0 + H_K \\
H_K &= -a \sqrt{\frac{2\pi}{K_{\rho}}} \frac{J_1^z}{\pi a} S_z \partial_x \theta_s(0) \\
&\quad + \frac{2J_2^z}{\pi a} S_z \sin \left(\sqrt{\frac{2\pi}{K_{\rho}}} \theta_a(0) \right) \sin \left(\sqrt{\frac{2\pi}{K_{\sigma}}} \phi_a(0) \right) \\
&\quad + \frac{J_1^{xy}}{\pi a} \left[S^- e^{-i \left(\sqrt{\frac{2\pi}{K_{\sigma}}} \phi_s(0) \right)} + \text{h.c.} \right] \cos \left(\sqrt{\frac{2\pi}{K_{\sigma}}} \phi_a(0) \right) \\
&\quad + \frac{J_2^{xy}}{\pi a} \left[S^- e^{-i \left(\sqrt{\frac{2\pi}{K_{\sigma}}} \phi_s(0) \right)} + \text{h.c.} \right] \cos \left(\sqrt{\frac{2\pi}{K_{\rho}}} \theta_a(0) \right), \\
H_0 &= \frac{v_F'}{2} \int dx \left[(\partial_x \phi_s)^2 + (\partial_x \theta_s)^2 + (\partial_x \phi_a)^2 + (\partial_x \theta_a)^2 \right] \tag{2}
\end{aligned}$$

with $K_{\rho} = 1/K_{\sigma} = K = \sqrt{\frac{1 + \frac{g_4}{2}\pi v_F - \frac{g_2}{2}\pi v_F}{1 + \frac{g_4}{2}\pi v_F + \frac{g_2}{2}\pi v_F}}$ being the Luttinger parameter, $v_F' = v_F \sqrt{(1 + \frac{g_4}{2}\pi v_F)^2 - (\frac{g_2}{2}\pi v_F)^2}$.

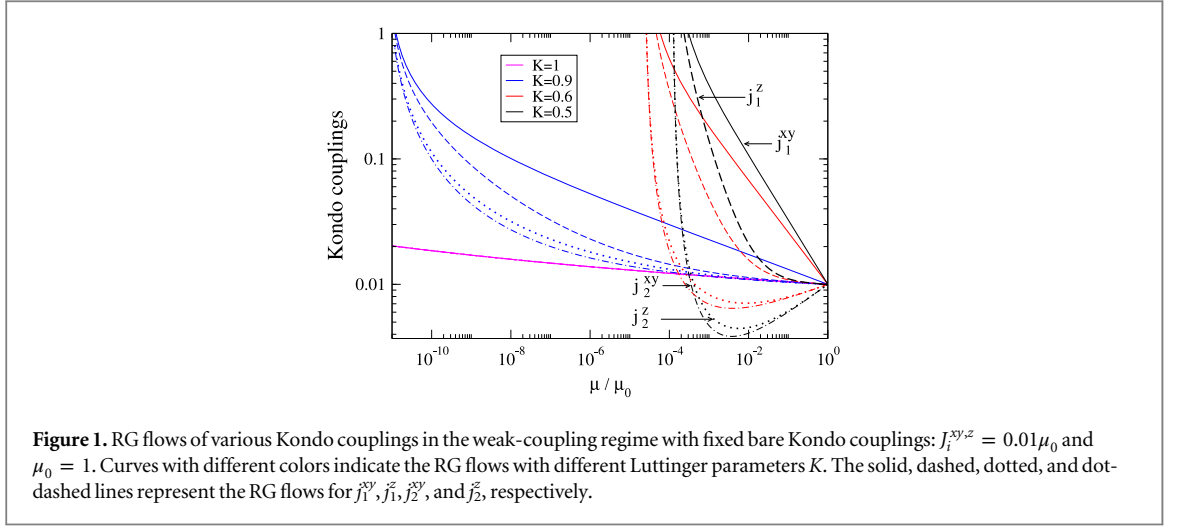
Here, we consider repulsive electron-electron interactions ($g_2, g_4 > 0$), giving $0 < K < 1$, and $K_{\rho(\sigma)}$ refers to the interaction strength in the charge (spin) sector. Note that the electron-electron interactions H_{int} term in equation (1) has been absorbed into the H_K term in equation (2) by re-scaling the boson fields mentioned above. Note also that $K_{\sigma} = 1, K_{\rho} < 1$ corresponds to a standard spinful Luttinger liquid with SU(2) spin symmetry; while $K_{\sigma} \neq 1$ when this symmetry is broken. The helical Luttinger lead we consider here corresponds to a spinful Luttinger liquid lead with broken SU(2) symmetry due to spin-orbit coupling with $K_{\rho} = K < 1$ and $K_{\sigma} = 1/K > 1$ (see [32]). Note that we have dropped the Klein factors in equation (2) as they can be included straightforwardly in the same manner as shown in [33, 34].

3. RG analysis of the model

3.1. RG analysis in weak coupling fixed point: $J_i^{xy,z} = 0$

3.1.1. RG scaling equations

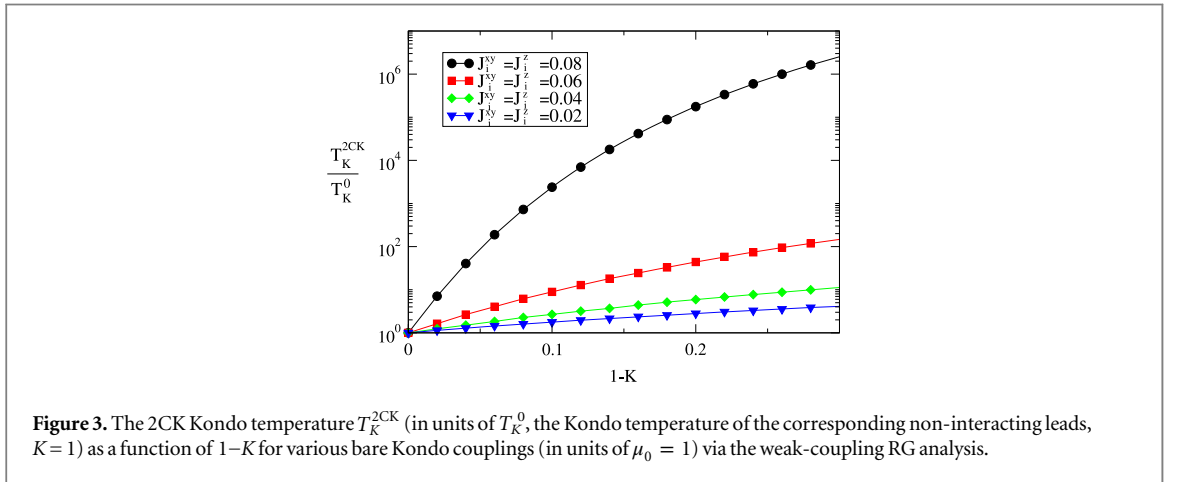
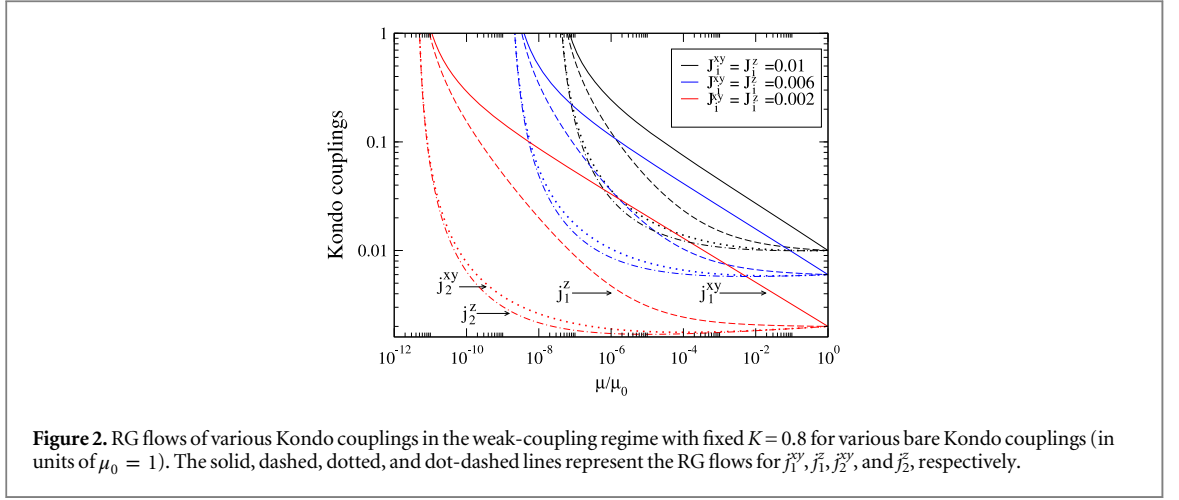
In the vicinity of the fixed point $J_i^{xy,z} = 0$, it has been shown in [29] that the scaling dimensions of these Kondo couplings based on the bosonized Hamiltonian equation (1) of [29] are: $[J_1^{xy}] = K < 1, [J_1^z] = 1, [J_2^{xy}] = [J_2^z] = \frac{1}{2}(K + \frac{1}{K}) > 1$ where $K < 1$ for repulsive electron interactions. Here, in our convention for scaling dimensions, relevant (irrelevant) operators carry the scaling dimensions of less (greater) than 1, while the



marginal operators carry scaling dimensions of exactly 1. The authors of [29] argued that for $K < 1$, under renormalization group (RG) transformations, the 2CK fixed point is reached as the relevant J_1 couplings flow to large values with decreasing temperatures; while the irrelevant J_2 couplings decrease to zero. However, for K being slightly less than 1, $K \rightarrow \Gamma^-$, via one-loop RG, beyond the bare scaling dimension analysis, we find it is possible that all four Kondo couplings flow to large values, depending on the values of K and the values of the bare Kondo couplings. This strongly indicates the existence of the 1CK fixed point in the parameter space of the model for $K < 1$. Following [33] and [31] via the renormalization group analysis of the bosonized Kondo model equation (2), the one-loop RG scaling equations in the limit of $K \rightarrow \Gamma^-$ read (see appendix A):

$$\begin{aligned}
 \frac{\partial j_1^{xy}}{\partial \ln \mu} &= (K - 1)j_1^{xy} - j_1^{xy}j_1^z - j_2^{xy}j_2^z, \\
 \frac{\partial j_1^z}{\partial \ln \mu} &= -(j_2^{xy})^2 - (j_1^{xy})^2, \\
 \frac{\partial j_2^{xy}}{\partial \ln \mu} &= \left[\frac{1}{2} \left(K + \frac{1}{K} \right) - 1 \right] j_2^{xy} - j_2^{xy}j_1^z - j_1^{xy}j_2^z, \\
 \frac{\partial j_2^z}{\partial \ln \mu} &= \left[\frac{1}{2} \left(K + \frac{1}{K} \right) - 1 \right] j_2^z - 2j_1^{xy}j_2^{xy}
 \end{aligned} \tag{3}$$

where μ is the running cutoff energy scale, and the dimensionless Kondo couplings are defined as: $j_1^{xy} \equiv \rho_0 \mu^{K-1} J_1^{xy}$, $j_1^z = \rho_0 J_1^z$, $j_2^{xy} = \rho_0 \mu^{\frac{1}{2}(K+\frac{1}{K})-1} J_2^{xy}$, and $j_2^z = \rho_0 \mu^{\frac{1}{2}(K+\frac{1}{K})-1} J_2^z$ with μ being a cutoff energy scale, and $\rho_0 = \frac{1}{\pi v_f} \equiv \frac{1}{2\mu_0}$ being the constant density of states for non-interacting leads ($K = 1$) and $\mu_0 = 1$ being the bandwidth of the conduction electrons in the leads. Note that the linear term in the above RG scaling equations comes from the nontrivial scaling dimensions of the corresponding Kondo couplings, while the quadratic terms in Kondo couplings are the corrections at one-loop order. For $K \rightarrow \Gamma^-$, both $J_2^{xy,z}$ terms are marginally irrelevant, $[J_2^{xy,z}] \rightarrow \Gamma^-$. Therefore, within the validity of perturbative RG, both $J_2^{xy,z}$ terms can still flow to a large value if bare Kondo couplings $J_i^{xy,z}$ are large enough (but they are still small, $J_i^{xy,z} = \mathcal{O}(1 - K) \ll 1$) or the electron interactions in the leads are weak enough, leading to (possibly) a 1CK fixed point (i.e. the quadratic terms overcome the linear term in RG equations). However, for small enough bare Kondo couplings (or strong enough interactions in the leads, $K \ll 1$), $J_2^{xy,z}$ terms are irrelevant and hence the system moves towards the 2CK fixed point. As shown in figure 1, in the relatively higher temperature (energy) regime $10^{-3} < \mu/\mu_0 < 1$, with decreasing K the system tends to flow to the 2CK fixed point where $j_1^{xy,z}$ flow to large values while $j_2^{xy,z}$ decreases with decreasing temperature (energy). However, for weak enough interactions in the leads, $K \rightarrow \Gamma^-$, all four Kondo couplings tend to flow to the 1CK fixed point with large values (see figure 1). A similar trend is found for a fixed $K \rightarrow 1$ and different bare Kondo couplings as shown in figure 2. It is therefore reasonable to expect a 1CK-2CK quantum phase transition in the parameter space of $J_{1,2}^{xy,z}$, K . However, the weak coupling RG analysis is valid only at relatively higher energies where all Kondo couplings remain small, $j_i^{xy,z} \ll 1$, and it breaks down as the system gets closer to the ground state where some Kondo couplings grow to the order of 1. As shown in figures 1 and 2, the energy range where $j_2^{xy,z}$ increases rapidly with a lowering energy scale already goes beyond the weak-coupling perturbative regime as j_1^{xy} already exceeds the perturbative regime at these scales, $j_1^{xy} > \mathcal{O}(1)$. In fact, the low energy behaviors are determined by the physics in the strong coupling regime. Therefore, to



address the possible quantum phase transition between the 1CK and 2CK fixed points, it is necessary to be able to access the neighborhood of the strong-coupling 2CK fixed point, as we shall discuss below.

3.1.2. 2-channel Kondo temperature T_K^{2CK}

To probe the crossover between 1CK and 2CK fixed points, it is instructive to investigate how the Kondo temperature T_K changes with increasing electron-electron interaction in the leads (or with the decreasing value of K from 1). Since J_1^{xy} becomes more relevant with decreasing K in the weak-coupling regime ($[J_1^{xy}] = K < 1$), it is expected that under RG the system first flows very quickly to the vicinity of the 2CK fixed point. As shown in figure 3, we find the Kondo temperature T_K^{2CK} associated with the 2CK fixed point, defined as the energy scale $\mu = T_K^{2CK}$ under RG where $j_1^{xy}, j_1^z \approx \mathcal{O}(1)$, increases rapidly with increasing electron interactions in the leads, and its value is much larger than the Kondo temperature of the same setup in the non-interacting limit ($K = 1$) T_K^0 , $T_K^{2CK} \gg T_K^0$. By contrast, in the case of a Kondo dot coupled to ordinary spinful Luttinger liquid leads in [25] and [23], J_1^{xy} is a marginal operator at tree level ($[J_1^{xy}] = 1$) in the weak-coupling limit; therefore, the 2CK energy scale T_K^{2CK} is much smaller than the Kondo scale for the corresponding non-interacting leads T_K^0 , $T_K^{2CK} \ll T_K^0$. Though the system in the weak coupling regime quickly approaches the strong-coupling 2CK fixed point as $\mu \rightarrow T_K^{2CK}$, the ultimate fate of the ground state depends on the RG flows of various Kondo couplings in the strong coupling regime, as discussed below.

3.2. RG analysis near the strong coupling (2CK) fixed point

3.2.1. RG scaling equations and the phase (RG flow) diagram

The authors of [29] performed scaling dimension analysis near a strong coupling regime where

$j_1^z = \mathcal{O}(1)$, $j_2^{xy,z} = j_1^{xy} = 0$. They performed the Emery–Kivelson unitary transformation [35] $U = e^{i\sqrt{2\pi}\phi S_z}$ on the bosonized Hamiltonian (equation (1) of [29]), and arrived at equation (2) of [29].

$$\begin{aligned}
H = H_0 - & \sqrt{\frac{2\pi}{K}} \delta J_1^z S_z \partial_x \theta_s(0) \\
& + \frac{2J_2^z}{\pi a} S_z \sin \left(\sqrt{\frac{2\pi}{K}} \theta_a(0) \right) \sin \left(\sqrt{2\pi K} \phi_a(0) \right) \\
& + (S^- + S^+) \left[\frac{J_1^{xy}}{\pi a} \cos \left(\sqrt{2\pi K} \phi_a(0) \right) \right. \\
& \left. + \frac{J_2^{xy}}{\pi a} \cos \left(\sqrt{\frac{2\pi}{K}} \theta_a(0) \right) \right]
\end{aligned} \tag{4}$$

with $\delta J_1^z = \frac{J_1^z}{\pi} - K\nu_F < 1$.

They found the scaling dimensions for the Kondo couplings to be $[J_1^{xy}] = \frac{K}{2}$, $[\delta J_1^z] = 1$, $[J_2^{xy}] = \frac{1}{2K}$, $[J_2^z] = \frac{1}{2}(K + \frac{1}{K})$. The J_1^{xy} term is relevant for $K < 2$, and the J_2^{xy} term is relevant for $\frac{1}{2} < K < 1$. For $K < 1$, this analysis shows that the J_1^{xy} term is the most relevant coupling, and it flows much faster than the J_1^z term to the strong-coupling 2CK fixed point where $j_1^{xy} \gg j_1^z \sim \mathcal{O}(1)$ (or $\delta j_1^z \ll 1$). However, as $K \rightarrow \Gamma$, the J_2^z term can flow to a large value towards the 1CK fixed point under one-loop RG if the bare Kondo couplings are large enough. This implies the existence of a stable 1CK near the strong coupling regime as all of the four Kondo couplings can either flow to or stay at large values (of order 1).

To gain more insight into the stability of the 1CK/2CK fixed point, we apply the RG approach at one-loop order together with bosonization and re-fermionization near the 2CK fixed point. First, we shall map the bosonized Hamiltonian equation (2) above (see [29]) onto an effective Kondo model via re-fermionization. It has been shown in [29] that near the strong coupling 2CK fixed point $j_1^{xy} \rightarrow \infty$, $j_1^z \rightarrow \mathcal{O}(1)$, $j_2^{z/xy} \rightarrow 0$, the effective Hamiltonian reads: $H_{2\text{CK}} = H_0 + \frac{2J_1^{xy}}{\pi a} S_x \cos(\sqrt{2\pi K} \phi_a(0))$. Note that the 2CK ground state in our system is a strong coupling fixed point ($j_1^{xy} \rightarrow \infty$), driven by electron-electron interactions (or Luttinger liquid physics) in the leads, similar to the 2CK fixed point in a Kondo dot coupled to two Luttinger liquid leads [23, 29] or to two metallic leads subject to an electromagnetic noise [34]. By contrast, the earlier version of the 2CK ground state in a magnetic impurity imbedded in non-interacting metals with two Kondo screening channels is an intermediate quantum critical fixed point, as suggested in [5, 14].

Near the 2CK fixed point, the dominating ‘backscattering’ J_1^{xy} term effectively cuts the Luttinger wire into two separate pieces [29, 31] at $x = 0$, leading to the well-known open boundary condition for an impurity in a Luttinger liquid at $x = 0$: $c_{i,R}(0) = -c_{i,L}(0)$ (or $\phi_{i,R}(0) = -\phi_{i,L}(0)$). Note that there are in total two such 2CK open boundary conditions in our two-lead setup as this condition holds for each lead separately. Note also that in general these conditions can be extended to $x \neq 0$: $\phi_{i,R}(x) = -\phi_{i,L}(-x)$ [31]. The boson field $\phi_a(0)$ is approximately pinned to a constant value [29], and so is the field $\phi_s(0)$. In fact, from the above 2CK open boundary conditions, we have $\phi_i(0) = \phi_{iL}(0) + \phi_{iR}(0) = 0$, and therefore $\phi_{a,s}(0) = 0$. Also, since S_x commutes with $H_{2\text{CK}}$, we may therefore set S_x to its eigenvalue $\pm \frac{1}{2}$ in $H_{2\text{CK}}$. As a result, the J_1^{xy} term in equation (4) can be regarded as a large fixed constant $J_{1,fix}^{xy}$ at the 2CK fixed point: $J_1^{xy} S_x \cos(\sqrt{2\pi K} \phi_a(0)) \sim J_{1,fix}^{xy}$ with $|J_{1,fix}^{xy}| \gg 1$, which effectively decouples the J_1^{xy} term from the rest of the terms in equation (4).

The stability of the 2CK fixed point should be analyzed via the deviation $\delta H_{2\text{CK}}$ from the fixed-point Hamiltonian $H_{2\text{CK}}$, described by the three remaining Kondo couplings (J_2^{xy} , δJ_1^z , J_2^z) near the 2CK fixed point (i.e. $\phi_a = 0$) in equation (4): $\delta H_{2\text{CK}} \equiv (H - H_{2\text{CK}})|_{2\text{CK}}$ (see [12]). The scaling dimensions of Kondo couplings near this 2CK fixed point at $j_1^{xy} \rightarrow \infty$, $j_1^z \rightarrow \mathcal{O}(1)$, $j_2^{z/xy} \rightarrow 0$ are [29, 31, 36] $[J_2^{xy}] = \frac{1}{K}$, $[\delta J_1^z] = 1 + \frac{1}{2K}$, $[J_2^z] = \frac{1}{K} + \frac{K}{2}$. Note that all the above three couplings are irrelevant for $K < 1$. This strongly indicates that the system favors the 2CK fixed point at ground state for $K < 1$. Meanwhile, by a stability analysis in section 4, we will show that the 2CK fixed point is also a stable fixed point for $K > \frac{1}{2}$ once the system approaches there (i.e. in the limit of $J_2^{xy} \rightarrow 0$). Therefore, the 2CK fixed point is really a strong-coupling fixed point, not an intermediate coupling fixed point since the latter case requires the existence of at least one relevant operator which drives the system from the intermediate 2CK fixed point to the ‘true’ strong coupling fixed point. But such relevant operators do not exist from the above scaling dimension analysis and that in section 4; all operators at the 2CK fixed point are irrelevant operators.

However, as shown in our weak-coupling RG analysis, the 2CK fixed point is unstable for $K \rightarrow \Gamma$ and/or large enough bare Kondo couplings such that $J_2^{xy,z}$ terms may become relevant again, and the system can undergo a 1CK-2CK quantum phase transition. To address this possibility, we shall focus below on the one-loop RG flows of the leading two irrelevant operators in $\delta H_{2\text{CK}}$ near the 2CK fixed point, given by (see equation (4)):

$$\delta H_{2\text{CK}} \approx \frac{J_2^{xy}}{\pi a} S^x \cos\left(\sqrt{\frac{2\pi}{K}} \theta_a(0)\right) - \sqrt{\frac{2\pi}{K}} \delta J_1^z S_z \partial_x \theta_s(0). \quad (5)$$

Note that we may consider the most relevant J_1^{xy} term to be the largest constant energy scale ($j_1^{xy} \rightarrow \infty$) we set at the stable 2CK fixed point. We estimate the small deviation in energy away from this fixed point for the other three Kondo couplings in equation (4). The bare scaling dimensions of these three remaining Kondo couplings are calculated based on the pinning of the J_1^{xy} term (or by setting $\cos(\sqrt{2\pi K} \phi_a) = \pm 1$) in equation (4). Therefore, we can estimate how irrelevant these three operators are relative to the 2CK fixed point with J_1^{xy} being fixed at infinity. Then we single out the two dominating irrelevant operators δJ_1^z and J_2^{xy} terms in $\delta H_{2\text{CK}}$ in equation (5). Finally, we study the stability of the 2CK fixed point due to these two terms.

To more effectively access the possible 1CK-2CK quantum critical point, we map the Hamiltonian near 2CK $H_0 + \delta H_{2\text{CK}}$ onto an effective Kondo model via re-fermionization subject to a bosonic environment [34]³:

$$\begin{aligned} H_0 + \delta H_{2\text{CK}} &\rightarrow H_0 + H'_0 + \delta H_{2\text{CK}} \\ &= \tilde{H}_0 + H_b + \tilde{H}_{2\text{CK}}, \end{aligned} \quad (6)$$

where

$$\begin{aligned} H'_0 &= \frac{v'_F}{2} \int dx (\partial_x \theta'_a)^2 \\ \tilde{H}_0 &= \frac{v'_F}{2} \int dx \left[2(\partial_x \theta_{0,a})^2 + (\partial_x \theta_{0,s})^2 \right. \\ &\quad \left. + (\partial_x \phi_s)^2 + (\partial_x \phi_a)^2 \right] \\ &= \sum_{k,\sigma,i=1(\tilde{L}),2(\tilde{R})} \epsilon(k) \tilde{c}_{k,i}^{\dagger\sigma} \tilde{c}_{k,i}^{\sigma} \end{aligned} \quad (7)$$

$$H_b = \frac{v'_F}{2} \int dx 2(\partial_x \tilde{\theta}_a)^2, \quad (8)$$

and

$$\begin{aligned} \tilde{H}_{2\text{CK}} &= J_2^{xy} S^- \left[s_{\tilde{L}\tilde{R}}^+ e^{i\sqrt{4\pi(\frac{1}{K}-1)} \tilde{\theta}_a(0)} + s_{\tilde{R}\tilde{L}}^+ e^{-i\sqrt{4\pi(\frac{1}{K}-1)} \tilde{\theta}_a(0)} \right] + \text{h.c.} \\ &\quad + \sqrt{\frac{\pi}{K}} \delta J_1^z (s_{\tilde{L}\tilde{L}}^z + s_{\tilde{R}\tilde{R}}^z) S_z. \end{aligned} \quad (9)$$

Here, the boson field θ'_a in H'_0 is decoupled from H_0 and is added here for the purpose of the mapping: it helps to map a Kondo dot coupled to interacting Luttinger liquid leads onto a Kondo dot coupled to non-interacting Fermi liquid leads subject to an Ohmic noisy boson environment. Similar mappings have been performed in earlier works (see, for example [3] and [34]) where in Kondo dot systems the equivalence between interactions in the Luttinger liquid leads and the bosonic (Ohmic) noisy environment has been established. Also, the effective non-interacting electron operator $\tilde{c}_{k,i}^{\sigma}$ is defined as:

$$\tilde{c}_{i=1(\tilde{L}),2(\tilde{R})}^{\uparrow(\downarrow)} = \frac{1}{\sqrt{2\pi a}} F_i^{\uparrow(\downarrow)} e^{\pm i(\sqrt{4\pi} \phi_{0,i}^{\uparrow(\downarrow)}(x) + k_F x)}. \quad (10)$$

with $i = 1(\tilde{L}), 2(\tilde{R})$ being the index for effective non-interacting left and leads, respectively,

$s_{\gamma\beta}^{\pm(z)} = \sum_{\alpha,\delta,k,k'} \frac{1}{2} \tilde{c}_{k\gamma}^{\dagger\alpha} \sigma_{\alpha\delta}^{\pm(z)} \tilde{c}_{k'\beta}^{\delta}$ being the spin-flip (z -component of the spin) operators between the effective

leads γ and β . Note that since the scaling dimension of $\cos(\sqrt{\frac{2\pi}{K}} \theta_a)$ at the 2CK fixed point in equation (9) is $\frac{1}{K}$ due to the open boundary condition [29], we have made the following decomposition for the boson field $\sqrt{\frac{1}{K}} \theta_a$:

$$\sqrt{\frac{1}{K}} \theta_a = \sqrt{2} \theta_{0,a} + \sqrt{2} \tilde{\theta}_a, \quad (11)$$

$$\sqrt{\frac{1}{K}} \theta'_a = \sqrt{2\left(\frac{1}{K} - 1\right)} \theta_{0,a} - \sqrt{\frac{2}{\frac{1}{K} - 1}} \tilde{\theta}_a, \quad (12)$$

³ Here, we drop the Klein factors in equation (5). Nevertheless, when including them in equation (5) (see appendix D), it is a straightforward task to arrive at equation (9) via re-fermionization equation (15).

where

$$\bar{\theta}_a = \sqrt{\frac{1}{K} - 1} \bar{\theta}_a. \quad (13)$$

Meanwhile, we set

$$\theta_s = \theta_{0,s}. \quad (14)$$

The re-fermionization of H_0 is done through the following identifications:

$$\begin{aligned} \sqrt{2} \theta_{0,a} &= \sqrt{2} (\phi_{0,1}^\uparrow + \phi_{0,2}^\downarrow) = -\sqrt{2} (\phi_{0,2}^\uparrow + \phi_{0,1}^\downarrow), \\ \sqrt{2} \theta_{0,s} &= -(\phi_{0,1}^\uparrow - \phi_{0,1}^\downarrow + \phi_{0,2}^\uparrow - \phi_{0,2}^\downarrow), \end{aligned} \quad (15)$$

where we have decomposed the boson field $\sqrt{\frac{1}{K}} \theta_a$ into two independent sets of boson fields: the ‘free’ ($\theta_{0,a}$) and ‘interacting’ ($\bar{\theta}_a$) parts. The ‘free’ part of the boson fields $\theta_{0,a}$ (defined in the same way as in section 2) can be re-fermionized into two effective non-interacting fermion leads described by \tilde{H}_0 where the electron destruction operator of the effective non-interacting leads \tilde{c}_i^σ is defined in equation (10). Note that in equation (15) the boundary conditions ($\phi_{0,i}^\uparrow(0) = -\phi_{0,i}^\downarrow(0)$) for each lead are imposed and implied; therefore the effective non-interacting leads \tilde{c}_i^σ also respect the 2CK open boundary condition ($\tilde{c}_i^\uparrow(0) = -\tilde{c}_i^\downarrow(0)$). Note also that due to the two 2CK boundary conditions, the fermionic degrees of freedom at $x = 0$ is reduced from four ($c_{i,R}, c_{i,L}$) to two, which is respected in both equation (5) and in the re-fermionized form, equation (6) via equation (15) and equation (10), as it should be. Meanwhile, the fields \tilde{c}_i also exhibit a helical nature: namely, the spin up/down ($\sigma = \uparrow/\downarrow$) electrons are tied to the right (R)/left (L) moving particles, respectively. The ‘free’ part of the boson field $\theta_{0,a}$ follows the correlations of the free fermions in 1D:

$$\left\langle e^{-i\sqrt{2\pi}\theta_{0,a}(t)} e^{i\sqrt{2\pi}\theta_{0,a}(0)} \right\rangle \propto \frac{1}{t}. \quad (16)$$

Meanwhile, the ‘interacting’ part of the boson field $\bar{\theta}_a$ acts as an effective dissipative ohmic boson environment (bath), represented by H_b . These bosons couple to the Kondo dot through the additional exponential ‘phase’ factors in the effective Kondo terms $\tilde{H}_{2\text{CK}}$, leading to all the combined Kondo–Luttinger physics [34]. In particular, since these dissipative ohmic bosons obey the following correlations via equation (9):

$$\left\langle e^{-i\sqrt{4\pi\left(\frac{1}{K}-1\right)}\bar{\theta}_a(t)} e^{i\sqrt{4\pi\left(\frac{1}{K}-1\right)}\bar{\theta}_a(0)} \right\rangle \propto \frac{1}{t^{2\left(\frac{1}{K}-1\right)}}; \quad (17)$$

while the impurity spin operator S_z exhibits the following correlation [29]:

$$\langle S_z(0) S_z(t) \rangle \propto \frac{1}{t^{\frac{1}{K}}}. \quad (18)$$

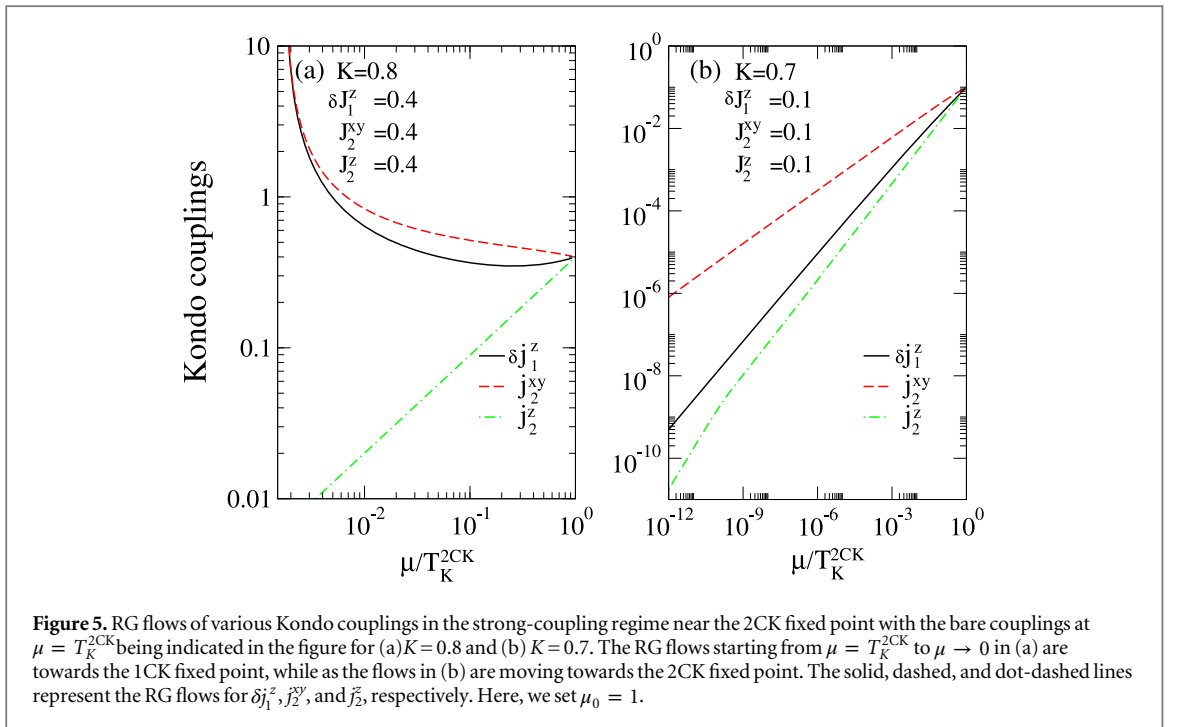
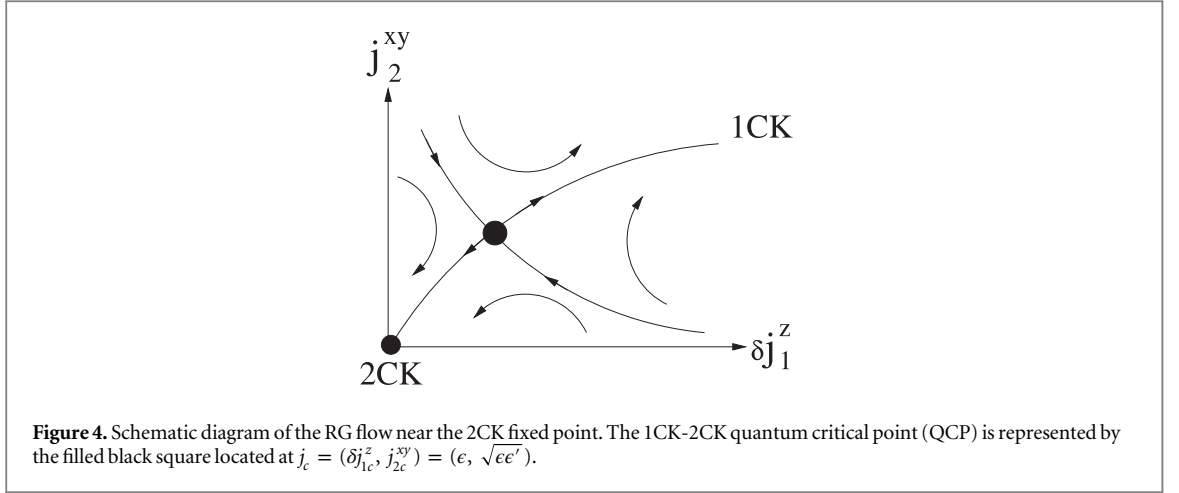
These correlations lead to the non-trivial bare scaling dimensions of the Kondo couplings and therefore to the first term (linear in the Kondo coupling) of the RG scaling equations. With the help of equation (11) to equation (15), we finally arrive at \tilde{H}_0 and $\tilde{H}_{2\text{CK}}$ in equation (9).

Next, we shall obtain the one-loop RG scaling equations for J_2^{xy} and δJ_1^z in equation (9). To this aim, we define the dimensionless couplings $j_2^{xy} \equiv \rho_0 \tilde{c}_2^\perp \mu^\epsilon J_2^{xy}(\mu)$ and $\delta j_1^z \equiv \rho_0 \tilde{c}_1^z \mu^{\epsilon'} \frac{\pi}{\sqrt{K}} \delta J_1^z(\mu)$ and $\epsilon \equiv \frac{1}{K} - 1$, $\epsilon' \equiv \frac{1}{2K}$ with $\tilde{c}_1^z, \tilde{c}_2^\perp$ being defined in appendix B and appendix C.

We derive the one-loop RG scaling equations via the poor-man’s scaling approach in [34] (see appendix B) and via the field-theoretical ϵ -expansion technique (see appendix C):

$$\begin{aligned} \frac{\partial j_2^{xy}}{\partial \ln \mu} &= \epsilon j_2^{xy} - j_2^{xy} \delta j_1^z, \\ \frac{\partial \delta j_1^z}{\partial \ln \mu} &= \epsilon' \delta j_1^z - (j_2^{xy})^2. \end{aligned} \quad (19)$$

Note that our RG analysis near the 2CK fixed point is performed for the Hamiltonian $\delta H_{2\text{CK}}$, the deviations from the 2CK fixed point where the J_1^{xy} term is not involved (see equations (4) and (5)). Therefore, unlike the RG equations in the weak-coupling limit shown in equation (3), here the $-(j_1^{xy})^2$ term is absent near the strong-coupling 2CK fixed point in the RG equation for δj_1^z in equation (19) as the J_1^{xy} term is pinned to a large constant value at the 2CK fixed point (see the paragraphs below equation (4)). Since the 2CK fixed point is shown to be a stable fixed point (see section 4 below), any small perturbations in $1/j_1^{xy}$ will not lead to the runaway flow from the 2CK fixed point.



Also, since both δj_1^z and j_2^{xy} terms fall into the perturbative regime, $\delta j_1^z, j_2^{xy} \ll 1$, our perturbative RG approach is therefore controlled. Upon solving for the RG equations in equation (19), for $K \rightarrow \Gamma$ we find an intermediate quantum critical fixed point (QCP) at $j_c \equiv (\delta j_{1,c}^z, j_{2,c}^{xy}) = (\epsilon, \sqrt{\epsilon\epsilon'})$ accessible by the perturbative RG approach, separating the 1CK fixed point (for $J \equiv (\delta J_1^z, J_2^{xy}) > J_c$) and the 2CK fixed point (for $J < J_c$) with j_2^{xy} and δj_1^z flowing towards a large ($J > J_c$) and vanishingly small ($J < J_c$) value, respectively (see figure 4). Here, J_c refers to the dimensionful bare critical Kondo coupling associated with j_c above. Note that though ϵ' approaches a finite non-vanishing value $1/2$ for $K \rightarrow 1$, our double- ϵ -expansion is still a controlled approach since all the critical properties are determined by the location of the QCP at $j_c = (\epsilon, \sqrt{\epsilon\epsilon'})$, which converges to 0 as $\epsilon \rightarrow 0$. This furthermore justifies the validity of our perturbative RG approach and the existence of the 1CK-2CK QCP in our model. To the best of our knowledge, this QCP may be regarded as the first realization of 1CK-2CK QPT that is accessible by a controlled theoretical approach. We would like to make a remark here regarding the quantum critical point in our model. Though we pointed out above that the 1CK-2CK QCP can be accessed via a controlled ϵ -expansion technique in the limit of $K \rightarrow \Gamma$, it exists in general in the multi-dimensional parameter space of $(J_1^{xy,z}, J_2^{xy,z}, K)$ with $K < 1$ (see equation (1)). Here, within the validity of the ϵ -expansion technique, we fix the Luttinger parameter $K \rightarrow \Gamma$ and investigate the QCP in the two-dimensional parameter space of $(\delta j_1^z, j_2^{xy})$ near 2CK fixed point.

The RG flows near the QCP are determined by linearizing the RG scaling equations as shown in figure 4. The typical RG flows corresponding to the 1CK and 2CK fixed points are shown in figures 5(a) and (b), respectively.

Note that $\delta j_1^z \rightarrow 0$ near the 2CK fixed point is equivalent to the original Kondo coupling j_1^z (see equation (4)) being at a large value (order of 1): $j_1^z \approx \mathcal{O}(1)$, consistent with the familiar 2CK fixed point with both $J_1^{xy,z}$ terms being large. However, we find the ‘1CK’ fixed point here in the strong-coupling analysis at one-loop order is somewhat different from the familiar (conventional) 1CK fixed point we obtained in the weak coupling regime where all the four Kondo couplings will flow to (or stay at) large values. Instead, our RG analysis based on re-fermionization for the coupling $j_2^z = \rho_0 \tilde{c}_2 \mu^{\frac{1}{k} + \frac{2}{k} - 1} J_2^z$ in equation (4) near the 2CK fixed point shows that it stays irrelevant up to one-loop order with the RG scaling equation:

$$\frac{\partial j_2^z}{\partial \ln \mu} = \left[\frac{1}{K} + \frac{K}{2} - 1 \right] j_2^z \quad (20)$$

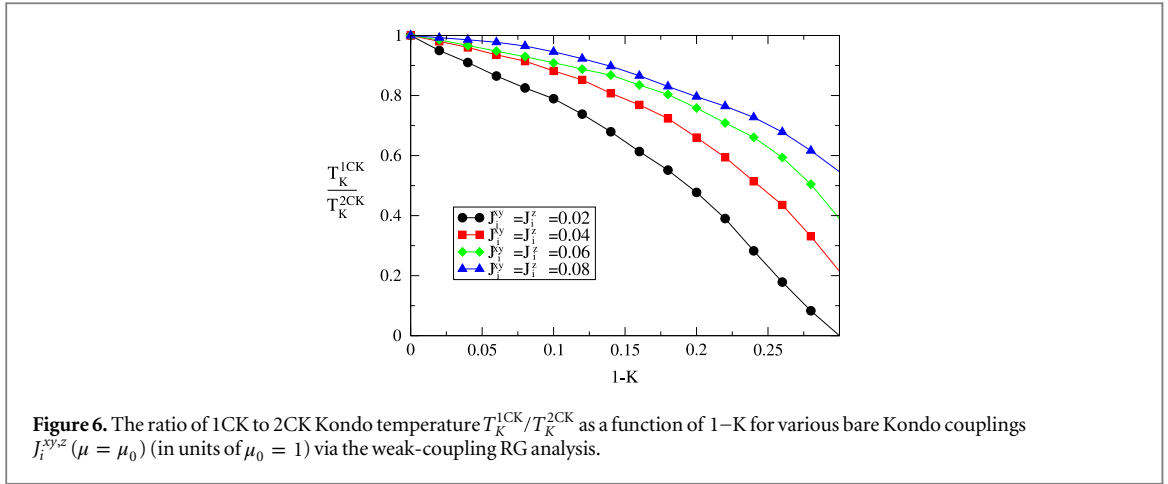
where we find no corrections at one-loop order. Note that unlike in the weak coupling RG where $j_1^{xy} j_2^{xy}$ will contribute to the one-loop renormalization of \tilde{j}_2^z (see equation (3)), the $j_1^{xy} j_2^{xy}$ term is absent here in equation (20) as j_1^{xy} has already been fixed at a very large value near the 2CK fixed point, $j_1^{xy}(T \approx T_K^{2CK}) \rightarrow j_{1,fix}^{xy} \gg 1$.

It is clear from equation (20) that [29] $j_2^z(\mu) \propto \mu^{\frac{1}{k} + \frac{K}{2} - 1}$, vanishing as $\mu \ll T_K^{2CK}$ even for $J > J_c$ where the system eventually flows to the 1CK fixed point (see figure 5). By combining the one-loop RG analysis in the weak and strong coupling limits, we may obtain the full crossover of \tilde{j}_2^z for the system which will eventually flow to the 1CK fixed point. For $T_K^{2CK} < T < \mu_0$, \tilde{j}_2^z first grows to the order of 1 (see figure 1), then it vanishes in a power-law fashion at lower temperatures $T \ll T_K^{2CK}$ (see figure 5). However, the above qualitative feature for \tilde{j}_2^z based on the one-loop RG analysis will get modified at the 2-loop order, where the relevant term $-(j_2^{xy})^2 j_2^z$ will be generated in equation (20) and drive \tilde{j}_2^z to a strong coupling fixed point, $j_2^z \rightarrow \infty$. In this case, the system flows to the conventional 1CK fixed point where all four Kondo couplings flow to the strong coupling fixed point. Therefore, we expect the linear conductance $G_{\perp}(T)$ contributed from \tilde{j}_2^z at the 1CK fixed point here to show the same temperature dependence as those in the isotropic one-channel Kondo system.

Here, we would like to make three remarks. Firstly, as a consistency check, via scaling dimension analysis we found the correlation functions for the leading two irrelevant operators near the 2CK fixed point, (defined as $\hat{\delta J}_1^z$ and \hat{J}_2^{xy} associated with the δJ_1^z and J_2^{xy} terms, respectively), in the bosonized Hamiltonian (see equation (5)) are kept the same, respectively, as that in the re-fermionized form (see equation (9)). To be more precise, in equation (5) $[J_2^{xy}] = 1/K$, $[\delta J_1^z] = 1 + \frac{1}{2K}$ [29]; therefore it follows $\langle \hat{J}_2^{xy}(\tau) \hat{J}_2^{xy}(0) \rangle \propto \frac{1}{\tau^{2/K}}$, and $\langle \hat{\delta J}_1^z(\tau) \hat{\delta J}_1^z(0) \rangle \propto \frac{1}{\tau^{2+1/K}}$. Similarly, we find from equation (9) that $[J_2^{xy}] = [s_{\Gamma R}^{\pm}] + [e^{i\sqrt{4\pi(\frac{1}{k}-1)}\theta_a(0)}] = 1 + (1/K - 1) = 1/K$ and $[\delta J_1^z] = [s_{\alpha\alpha}^z] + [S_z] = 1 + \frac{1}{2K}$, the same as those obtained from equation (5), respectively. Therefore, the correlation functions for the \tilde{j}_2^z and δJ_1^z terms are kept in the same form before (equation (5)) and after (equation (9)) the re-fermionization mapping is performed, as expected.

Secondly, we have checked that the RG scaling equations near the 2CK equation (19) via re-fermionization are reproducible via the similar RG approach based directly on the bosonized Hamiltonian equation (5) without going through re-fermionization (see appendix D). Nevertheless, let us emphasize here again that it is technically more advantageous and physically more transparent to address the quantum critical properties near 1CK-2CK QPT within the fermionic effective Kondo model as there are well-established field-theoretical approaches, such as perturbative RG combined with the field-theoretical ϵ -expansion technique. Though one can access the quantum criticality in our system via the bosonized version in equation (5), the controlled theoretical approaches to access the quantum criticality of our model system via equation (5) are either absent or obscure. The derivation of the RG scaling equations, equation (19), shown in appendix D offers an independent check of our re-fermionization mapping and the quantum critical properties obtained via the effective Kondo model in equation (9).

Finally, within the perturbative RG approach, the one-loop corrections can in general be added to the scaling dimension analysis in the RG scaling equations. This has been demonstrated in the weak-coupling limit of our model (see appendix A and references [33] and [31]). In fact, this approach has also been widely used in various related models, such as in the Kondo–Luttinger system in [9], in pseudogap Kondo problems in [39–41, 43], and [45], and in the dissipative Kondo quantum dot system in [34]. Near the strong-coupling 2CK fixed point of our model, we argue that one-loop perturbative RG contributions can still be added to our scaling dimension analysis at the 2CK fixed point as (1) the \tilde{j}_1^{xy} term is absent in RG equation, equation (19), (2) near 2CK the bare and renormalized leading irrelevant Kondo couplings \tilde{j}_2^{xy} and δj_1^z are both within the perturbative (weak-coupling) regime, j_2^{xy} , $\delta j_1^z \ll 1$, and (3) the location of our QCP j_c separating the 1CK and 2CK fixed points is still in the weak-coupling regime where the perturbative RG approach is valid. Therefore, our perturbative one-loop RG approach is controlled and is applicable for analyzing the stability of the 2CK fixed point.



However, the Emery–Kivelson unitary transformation that we applied in section 3.2, taking our Hamiltonian from the weak-coupling limit equation (2) to the strong coupling regime in equation (19) (see [29]), is a non-perturbative approach. Nevertheless, once we arrive near the strong-coupling 2CK described by δH_{2CK} , the rest of the RG analysis is perturbative and controlled.

3.2.2. 1-channel Kondo temperature T_K^{1CK}

As mentioned above, for $J > J_c$ with decreasing temperature the system crosses over from the 2CK to the 1CK fixed point at a much lower energy scale $\mu \approx T_K^{1CK} \ll T_K^{2CK}$ where T_K^{1CK} refers to the Kondo temperature associated with the 1CK fixed point. As shown in figure 6, the 1CK fixed point persists to be the ground state at a finite but weak electron-electron interaction strength, $K_c < K < 1$ with K_c being the critical interaction below which the ground state switches from the 1CK to the 2CK fixed point. Meanwhile, the crossover scale to the 1CK fixed point T_K^{1CK} (with respect to T_K^{2CK}) for $J > J_c$ gets reduced significantly as interaction gets stronger. Also, for a fixed value of K , the ratio T_K^{1CK}/T_K^{2CK} is larger for larger bare Kondo couplings J , as expected.

4. Stability analysis of the 1CK and 2CK fixed points for $K < 1$

Having found the possible QPT between the 1CK and 2CK fixed points, it is important to perform a stability analysis and study how robust the quantum critical point of our system is against small perturbations. Equivalently, we need to know how stable the 1CK and 2CK fixed points are for $K < 1$.

We first examine the stability of the helical Luttinger liquid lead itself. In general there exists the single particle backscattering term due to the interaction of $c_{i,R/L}(0)$ and the quantum dot [29]: $t' c_{i,R}^\dagger c_{i,L} + \text{h.c.}$. However, this term is forbidden here as it breaks time-reversal symmetry. Meanwhile, for the 1D Hubbard model in general there exists the ‘spin-flip’ backscattering term in H_u of the form $H_{sf} \propto c_{i,L}^\dagger c_{i,L}^\dagger c_{i,R}^\dagger c_{i,R} + \text{h.c.}$. However, due to the helical nature of our leads (or the right/left moving electrons are tied to their spins, i.e. only $c_{R(L)}^{\uparrow(\downarrow)}$ electrons exist), this H_{sf} term is therefore absent. Nevertheless, at half-full, the Umklapp term that exists on a single bond is allowed by the time-reversal symmetry [28]:

$$H_{um} = g_u c_R^{\dagger\uparrow}(0) c_R^{\dagger\downarrow}(0) c_L^\downarrow(0) c_L^\uparrow(0) + \text{h.c.} \quad (21)$$

The scaling dimension of this term has been shown to be $[H_{um}] = 4K$, indicating that the helical edge state is unstable towards an insulating phase for $K < \frac{1}{4}$. Note that for the band away from half-full, the Umklapp term vanishes [31].

We now focus on the effects of the particle-hole (p-h) asymmetry on the stability of these two fixed points as indicated in [23, 34] and [25] that it is the most relevant perturbation for a Kondo dot coupled to Luttinger liquid leads. Let us first address this issue at the 2CK fixed point where the two leads are effectively disconnected. The particle-hole asymmetry in our Kondo model generates potential scattering terms of the following form [23]:

$$\begin{aligned}
H_{1ps} &= H_t + H_{t_e}, \\
H_t &= t \sum_{k,i,\sigma,\alpha=L,R} c_{k,i}^{\dagger\sigma\alpha} c_{k,i}^{\sigma\alpha}, \\
H_{t_e} &= t_e \sum_{k,i \neq j, \sigma} c_{k,i}^{\dagger\sigma\alpha} c_{k,j}^{\sigma\alpha} + \text{h.c.}
\end{aligned} \tag{22}$$

with $i, j = 1(\tilde{L}), 2(\tilde{R})$ being the lead index, $\sigma = \uparrow$ (R), \downarrow (L) being spin index, and R(L) being the right (left) moving particles. Here, t and t_e terms represent a chemical potential of each lead and a weak tunneling between the disconnected Luttinger leads [32]. Meanwhile, two additional two-particle scattering terms H_{2p} involving tunneling of spin (t_σ) and of charge (t_ρ) can be generated by the weak tunneling t_e via 2nd-order perturbation (see figures 2(d)–(f) of [32]), given by:

$$\begin{aligned}
H_{2ps} &= H_{t_\sigma} + H_{t_\rho}, \\
H_{t_\sigma} &= t_\sigma \sum_k c_{k,1}^{\dagger\uparrow R} c_{k,2}^{\uparrow R} c_{k,2}^{\dagger\downarrow L} c_{k,1}^{\downarrow L} + \text{h.c.}, \\
H_{t_\rho} &= t_\rho \sum_k c_{k,1}^{\dagger\uparrow R} c_{k,2}^{\uparrow R} c_{k,1}^{\dagger\downarrow L} c_{k,2}^{\downarrow L}.
\end{aligned} \tag{23}$$

The bosonized form of equation (23) reads [32]:

$$\begin{aligned}
H_{1ps} + H_{2ps} &= t \frac{K}{2\pi a} \partial_x \phi_s + \frac{t_e}{2\pi a} \cos(\sqrt{2\pi K} \phi_a(0)) \cos\left(\sqrt{\frac{2\pi}{K}} \theta_a(0)\right) \\
&\quad + \frac{t_\rho}{2\pi a} \cos(2\sqrt{2\pi K} \phi_a) + \frac{t_\sigma}{2\pi a} \cos\left(2\sqrt{\frac{2\pi}{K}} \theta_a\right).
\end{aligned} \tag{24}$$

Near 2CK, $\phi_a(0)$ is a constant, therefore the scaling dimensions of these term gives: $[t] = 1, [t_e] = \frac{1}{2K}, [t_\sigma] = \frac{2}{K}$ ($t_\rho \approx \text{const.}$) [32]. It is clear that all operators are irrelevant for $\frac{1}{2} < K < 2$; the t_e term becomes relevant for $K < \frac{1}{2}$, and t_σ is relevant for $K > 2$.

Next, we consider the stability of the 1CK fixed point. Since the cross-channel Kondo coupling $J_2^{\sigma\gamma}$ term flows under RG along with $J_1^{\sigma\gamma}$ to large values while as J_1^z stays at order of 1, the two semi-infinite Luttinger wires are joined into one single infinite Luttinger wire [25]. In contrast to the ‘weak tunneling’ processes mentioned above at the 2CK fixed point, the potential scattering term generates the ‘weak backscattering’ processes between the electrons in the upper and lower edges, including the single-particle backscattering term v_e , and the two-particle backscattering terms v_ρ , and v_σ (see figures 2(a)–(c) in [32]):

$$\begin{aligned}
H_{v_e} &= v_e \sum_k c_{k,1}^{\dagger\uparrow R} c_{k,2}^{\uparrow L} + c_{k,1}^{\dagger\downarrow L} c_{k,2}^{\downarrow R} + \text{h.c.}, \\
H_{v_\rho} &= v_\rho \sum_k c_{k,1}^{\dagger\uparrow R} c_{k,2}^{\uparrow L} c_{k,1}^{\dagger\downarrow L} c_{k,2}^{\downarrow R} + \text{h.c.}, \\
H_{v_\sigma} &= v_\sigma c_{k,1}^{\dagger\uparrow R} c_{k,2}^{\uparrow L} c_{k,2}^{\dagger\downarrow R} c_{k,1}^{\downarrow L} + \text{h.c.}
\end{aligned} \tag{25}$$

In fact, there exists a duality mapping between the ‘weak tunneling’ and ‘weak backscattering’ limits [32]: $c_{k,2}^{\uparrow R} \rightarrow c_{k,2}^{\uparrow L}, c_{k,2}^{\downarrow R} \rightarrow c_{k,2}^{\downarrow L}, t_e \rightarrow v_e, t_\rho \rightarrow v_\rho, t_\sigma \rightarrow t_\rho, K \rightarrow \frac{1}{K}$. Note that at the 1CK fixed point, ϕ_a is not pinned to a constant as opposed to that in the 2CK case. The scaling dimensions of these terms can be read off straightforwardly [32]: $[v_e] = \frac{1}{2}(K + \frac{1}{K}), [v_\rho] = 2K$, and $[v_\sigma] = \frac{2}{K}$. The v_e term is always irrelevant for $K < 1$, while the v_ρ and v_σ terms are irrelevant for $\frac{1}{2} < K < 2$ and relevant otherwise.

Based on the above analysis, we find that both the 1CK and 2CK fixed points are stable for $\frac{1}{2} < K < 1$, and unstable for $K < \frac{1}{2}$. We have checked that our analysis reproduces the well-known results for a Kondo dot coupled to conventional Luttinger liquid leads in [23], [25] and [34] where $[t_e] = \frac{1}{2K}$ at the 2CK fixed point and $[v_e] = \frac{1}{2}(1 + K)$ at the 1CK fixed point.

As a final remark, we consider here the parity (left-right) symmetric model where $J_L = J_{LL} = J_{RR}$ with $J_{LL(RR)}$ being referred to as the Kondo couplings involving only the left (right) lead. Nevertheless, parity asymmetry is a relevant perturbation near the 2CK fixed point. In the presence of parity asymmetry ($J_{LL} \neq J_{RR}$), the system will flow to the 1CK fixed point with the large bare Kondo couplings [34].

5. Critical properties near the 1CK-2CK quantum phase transition

The critical properties and crossovers of various thermodynamical quantities near this newly found 1CK-2CK QCP can be obtained via the above RG approach combined with the field-theoretical ϵ -expansion technique [37–41]. We employ here a double- ϵ -expansion with two small expansion parameters ϵ and ϵ' . Our approach leads to more accurate results for the Luttinger parameter $K \rightarrow \Gamma$. Note that though ϵ' approaches a finite non-vanishing value $1/2$ for $K \rightarrow 1$ instead of zero, our double- ϵ -expansion is still a controlled approach since all the critical properties are determined by the location of the QCP $j_c = (\epsilon, \sqrt{\epsilon\epsilon'})$, which converges to 0 as $\epsilon \rightarrow 0$. Following references [39–41], we define the renormalized pseudo-fermion fields \tilde{f}_σ and the renormalized dimensionless Kondo couplings j as: $f_\sigma = \sqrt{Z_f} \tilde{f}_\sigma$, and $J_2^{xy} = \frac{\mu^{-\epsilon} Z_f^\perp j_2^{xy}}{\epsilon_1^\perp Z_f}$, $\delta J_1^z = \frac{\mu^{-\epsilon'} Z_f^z \sqrt{K}}{\epsilon_1^z Z_f} \delta j_1^z$ with Z_f and $Z_f^{\perp/z}$ being the renormalization factors for the impurity field and Kondo couplings, respectively and μ is a renormalization energy scale. The renormalization factors are obtained via minimal subtractions of poles [39, 40], given by (see appendix C):

$$\begin{aligned} Z_{j^\perp} &= 1 + \frac{\delta j_1^z}{\epsilon'}, \\ Z_{j^z} &= 1 + \frac{(j_2^{xy})^2 / \delta j_1^z}{2\epsilon}, \\ Z_f &= 1 + \frac{(j_2^{xy})^2}{8\epsilon} + \frac{(\delta j_1^z)^2}{16\epsilon'}. \end{aligned} \quad (26)$$

Within the field-theoretical RG approach, we have checked that the RG scaling equations in equation (19) can be reproduced via calculating the β -functions: $\beta(j_i) \equiv \mu \frac{\partial j_i}{\partial \mu} |_{j_i,0}$ with μ being an energy scale, $j_i = j_2^{xy}$, δj_1^z being the renormalized Kondo couplings and $J_{1,0} = \delta J_1^z$, $J_{2,0} = J_2^{xy}$ being the bare Kondo couplings (see appendix C). Below we discuss various critical properties and crossover functions based on the field-theoretical ϵ -expansion approach.

5.1. Observables at criticality

We first calculate various observables at criticality, including correlation length exponent, impurity entropy, dynamical properties of the T-matrix and local spin susceptibility.

5.1.1. Correlation length exponent ν

The correlation length exponent ν describes how the correlation length ξ diverges when the system is tuned to the transition: $\xi \propto |t|^{-\nu}$ with $t \equiv \frac{J - J_c}{J_c}$ being the dimensionless distance to the QCP. It also gives the power-law vanish of the characteristic crossover energy scale T^* close to the transition: $T^* \propto \mu |t|^\nu$. To calculate ν , we first linearize the RG scaling equations equation (19) near QCP. The correlation length exponent ν is determined by the largest eigenvalue of the coupled linearized equations, found to be:

$$\nu = \frac{4K}{\sqrt{1 + 16K\epsilon} - 1} = \frac{1}{2\epsilon} + \mathcal{O}(1) + \mathcal{O}(\epsilon^2, \epsilon'^2) \quad (27)$$

where the leading order behavior $\nu \approx \frac{1}{2\epsilon}$ is obtained by expanding the square-root in equation (27) in the limit of $\epsilon \ll \epsilon'$.

5.1.2. Impurity entropy

The impurity contribution to the low-temperature entropy near QCP is obtained by a perturbative calculation of the impurity thermodynamic potential Ω_{imp} with respect to the 2CK fixed point and taking the temperature derivative [40]: $S_{\text{imp}} = \frac{\partial \Omega_{\text{imp}}}{\partial T}$. At QCP and $T = 0$ it can be written as:

$$S_{\text{imp}}^{\text{QCP}} = S_{\text{imp}}^{\text{2CK}} + \Delta S_{\text{imp}}. \quad (28)$$

where $S_{\text{imp}}^{\text{2CK}} = \ln \sqrt{2K} = \frac{1}{2} \ln 2K$ is the zero-temperature residual impurity entropy at 2CK fixed point which shows the existence of fractionally degenerate ground state [15, 16, 29], and ΔS_{imp} is the correction to $S_{\text{imp}}^{\text{2CK}}$ at QCP. Following similar renormalized perturbative calculations in [40], we find

$$\Delta S_{\text{imp}} = \pi^2 \ln 2 \left[\frac{\epsilon \left(j_{2c}^{xy} \right)^2}{4} + \frac{\epsilon' \left(\delta j_{1c}^z \right)^2}{8} \right] = \frac{3\epsilon^2 \pi^2 \ln 2}{32K}. \quad (29)$$

Therefore, we have:

$$S_{\text{imp}}^{\text{QCP}} = \frac{1}{2} \ln 2K + \frac{3\epsilon^2 \pi^2 \ln 2}{32K}. \quad (30)$$

5.1.3. The T -matrix

The conduction electron T -matrix, $T_{\alpha\alpha'}(\omega)$, in the Kondo model carries important information on the scattering of the conduction electrons from lead α to lead α' via the impurity. In particular, $T_{\alpha\alpha'}(\omega)$ with $\alpha \neq \alpha'$ describes the transport across the dot, detectable in transport measurements. The T -matrix is determined from the conduction electron Green functions [42]: $G_{\alpha\alpha'}(t) = \langle c_{\alpha}(0) c_{\alpha'}^{\dagger}(t) \rangle$ through

$G_{\alpha\alpha'} = G_{\alpha\alpha'}^0 \delta_{\alpha\alpha'} + G_{\alpha\alpha}^0(\omega) T_{\alpha\alpha'}(\omega) G_{\alpha'\alpha'}^0(\omega)$. Near the 2CK fixed point, $T_{\alpha\alpha'}(\omega)$ with $\alpha \neq \alpha'$ is defined through the propagator, G_T , of the composite operator $T_{\alpha\alpha} = J_2^{xy} e^{i\sqrt{4\pi(\frac{1}{k}-1)}\theta_a(0)} f_{\sigma}^{\dagger} f_{\sigma'} \tilde{c}_{\alpha}^{\sigma'}$ (see equation (9)): $T_{\alpha\alpha'}(\omega) = G_T(\omega)$ [40].

Following the similar calculations in [40] and appendix C, we analyze the propagator $G_T(\omega)$ near the 2CK fixed point and find at zero temperature $\text{Im}(T_{\alpha\alpha'}^{2\text{CK}}(\omega)) \propto \frac{1}{\omega^{-\eta_T^{2\text{CK}}}}$ with the anomalous exponent at the tree level with respect to the 2CK fixed point given by $\eta_T^{2\text{CK}} = 2\epsilon$ (i.e. $\text{Im}(T_{\alpha\alpha'}^{2\text{CK}}(\omega)) \propto \omega^{2\epsilon}$). Near 1CK-2CK QCP, however, $\text{Im}(T_{\alpha\alpha'}(\omega))$ acquires an additional anomalous power-law behavior:

$$\text{Im}(T_{\alpha\alpha'}(\omega)) \propto \frac{1}{\omega^{-\eta_T^{2\text{CK}} - \eta_T}} \quad (31)$$

where the additional anomalous exponent η_T is obtained via the renormalization factor Z_T for the T -matrix propagator $T_{\alpha\alpha'}(\omega)$ [39, 40]: $\eta_T = \beta(j_2^{xy}) \frac{\partial \ln Z_T}{\partial j_2^{xy}} \Big|_j + \beta(\delta j_1^z) \frac{\partial \ln Z_T}{\partial \delta j_1^z} \Big|_j$. Here, the renormalization factor Z_T is obtained by minimal subtraction of poles [39, 40]: $Z_T = \frac{Z_f^2}{Z_j^{\perp}}$ with $Z_{\beta} Z_{j^{\perp}}$ given by equation (26). We find therefore

$$\eta_T = \frac{\left(j_{2c}^{xy} \right)^2}{2} - 2\delta j_{1c}^z + \frac{\left(\delta j_{1c}^z \right)^2}{4} = \frac{\epsilon}{4K} - 2\epsilon + \frac{\epsilon^2}{4}, \quad (32)$$

and $\text{Im}(T_{\alpha\alpha'}(\omega))$ at QCP behaves as:

$$\text{Im}(T_{\alpha\alpha'}(\omega)) \propto \omega^{\frac{\epsilon}{4K} + \frac{\epsilon^2}{4}}. \quad (33)$$

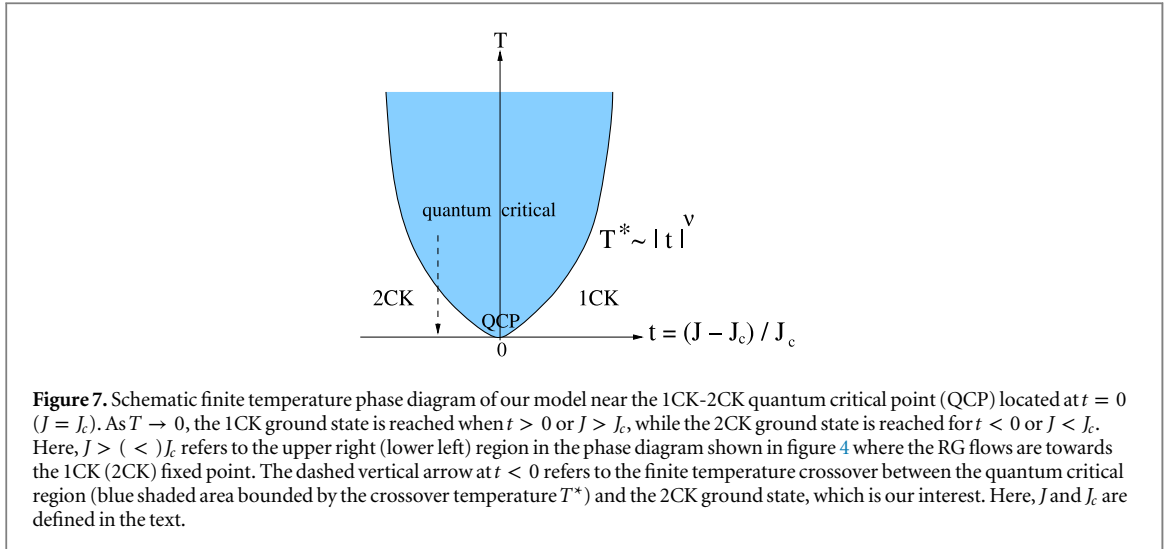
5.1.4. Local spin susceptibility $\chi_{zz}(\omega)$

The local dynamical spin susceptibility $\text{Im}(\chi_{zz}(\omega))$ at the impurity (quantum dot) is defined as the time Fourier transform of the spin-spin correlator: $\langle S_z(0) S_z(t) \rangle$. At zero temperature, the imaginary part of the local susceptibility, $\text{Im}(\chi_{zz}(\omega))$, shows a power-law behavior at QCP:

$$\text{Im}(\chi(\omega)_{\text{QCP}}) \propto \frac{1}{\omega^{-\eta_{\chi}^{2\text{CK}} - \eta_{\chi}}}. \quad (34)$$

Here, $\eta_{\chi}^{2\text{CK}} = \epsilon$ is the anomalous exponent of $\text{Im}(\chi_{zz}(\omega))$ at the tree level with respect to the 2CK fixed point via the correlator $\langle S_z(0) S_z(t) \rangle \propto \frac{1}{t^{\frac{1}{k}}}$ evaluated at the 2CK fixed point [29] (i.e. $\text{Im}(\chi_{zz}^{2\text{CK}}(\omega)) \propto \omega^{\epsilon}$), and η_{χ} is the correction to the anomalous exponent $\eta_{\chi}^{2\text{CK}}$ when the system is at QCP. Via ϵ -expansion within the field-theoretical RG framework [39, 40], η_{χ} reads: $\eta_{\chi} = \beta(j_2^{xy}) \frac{\partial \ln Z_{\chi}}{\partial j_2^{xy}} \Big|_{j_2^{xy}, \delta j_{1c}^z} + \beta(\delta j_1^z) \frac{\partial \ln Z_{\chi}}{\partial \delta j_1^z} \Big|_{j_2^{xy}, \delta j_{1c}^z}$ with $Z_{\chi} = Z_f^2$ being the renormalization factor for the impurity susceptibility [39, 40] and Z_f defined in equation (26). Carrying out the above calculations, we arrive at

$$\eta_{\chi} = \frac{\left(j_{2c}^{xy} \right)^2}{2} + \frac{\left(\delta j_{1c}^z \right)^2}{4} = \frac{\epsilon}{4K} + \frac{\epsilon^2}{4}, \quad (35)$$



and finally $\text{Im}(\chi_{zz}^{2\text{CK}}(\omega))$ at QCP shows the following power-law behaviors:

$$\text{Im}(\chi_{zz}(\omega)) \propto \omega^{\epsilon + \frac{\epsilon}{4K} + \frac{\epsilon^2}{4}}. \quad (36)$$

5.2. Hyperscaling

The impurity correlations at QCP are expected to obey certain hyperscaling properties. For example, the local dynamic spin susceptibility at criticality obeys $\frac{\omega}{T}$ scaling in the following form [39–41, 43]:

$$\text{Im}(\chi_{loc}(\omega, T)) = \frac{\mathcal{A}}{\omega^{-\eta_\chi^{2\text{CK}} - \eta_\chi}} \Phi\left(\frac{\omega}{T}\right) \quad (37)$$

with $\Phi(\frac{\omega}{T})$ being a universal crossover function for the QCP here and \mathcal{A} being a non-universal pre-factor. Similar scaling form can be found in the T-matrix. Hyperscaling can be used to determine relations between various critical exponents. It has been known [39–41, 43] that the correlation length exponent ν and the anomalous exponent η_χ are sufficient to determine all critical exponents associated with a local field h . In particular, the exponents γ and γ' via the $T \rightarrow 0$ limit of the local susceptibility near criticality are defined as [41, 43]:

$$\begin{aligned} \chi_{loc}(t < 0; T = 0) &\propto (-t)^{-\gamma}, & \gamma &= \nu(1 - \eta_\chi), \\ T\chi_{loc}(t > 0; T = 0) &\propto t^{\gamma'}, & \gamma' &= \nu\eta_\chi. \end{aligned} \quad (38)$$

Meanwhile, the critical exponents β and δ associated with the local magnetization m_{loc} can be determined by [41, 43]:

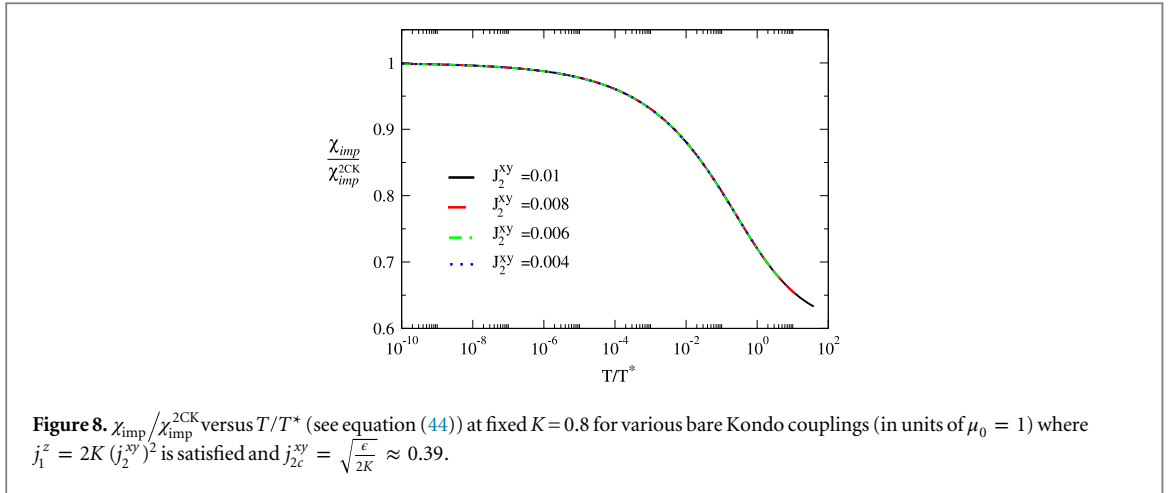
$$\begin{aligned} m_{loc}(t > 0; T = 0) &\propto t^\beta, & \beta &= \frac{1}{2}\nu\eta_\chi, \\ m_{loc}(t = 0, T = 0) &\propto |h|^\delta, & \delta &= \frac{2}{\eta_\chi} - 1. \end{aligned} \quad (39)$$

With the values for critical exponents ν (equation (27)) and η_χ (equation (35)) at hand, the other critical exponents are therefore given by:

$$\begin{aligned} \gamma &= \frac{1}{2\epsilon} - \frac{1 + K\epsilon}{8K} + \mathcal{O}(\epsilon^2, \epsilon'^2), & \gamma' &= \frac{1 + K\epsilon}{8K} + \mathcal{O}(\epsilon^2, \epsilon'^2), \\ \beta &= \frac{1 + K\epsilon}{16K} + \mathcal{O}(\epsilon^2, \epsilon'^2), & \delta &= \frac{8K}{\epsilon + K\epsilon^2} - 1 + \mathcal{O}(\epsilon^2, \epsilon'^2). \end{aligned} \quad (40)$$

5.3. Crossover near critical point

Next, we focus on calculating the crossover functions close to the 1CK-2CK quantum critical point. In general, the crossover functions of observables near criticality depend on the RG flows of both δj_1^z and j_2^{xy} (see figure 7); therefore they may not be expressed analytically in terms of universal crossover functions of a single variable. Nevertheless, great progress can be made when one makes a special choice of bare (initial) values of Kondo



couplings such that $\epsilon' \delta j_1^z = (J_2^{xy})^2$. Note that this set of bare couplings can in general be tuned through adjusting various microscopic parameters, such as spin-orbit coupling in 2DTIs, and the lead-dot hopping. For this particular choice of bare couplings, we found and checked that the RG flows of $\delta j_1^z(\mu)$ and $j_2^{xy}(\mu)$ follow the well-approximated trajectory: $\epsilon' \delta j_1^z \approx (j_2^{xy})^2$, (i.e. $\beta(\delta j_1^z) \approx 0$). Under this constraint, only one RG β -function ($\beta(j_2^{xy})$) effectively remains:

$$\beta(j_2^{xy}) = \epsilon j_2^{xy} - 2K (j_2^{xy})^3. \quad (41)$$

One can therefore easily solve equation (41) analytically, and its solution for the range between QCP at $j_{2c}^{xy} = \sqrt{\frac{\epsilon}{2K}} = \sqrt{\epsilon \epsilon'}$ and the 2CK fixed point ($j_2^{xy} < j_{2c}^{xy}$ where our RG and ϵ -expansion approach is controlled) is found to be:

$$j_2^{xy}(\mu) = \frac{j_{2c}^{xy}}{\sqrt{1 + \left(\frac{\mu}{T^*}\right)^{-2\epsilon}}} \quad (42)$$

where $T^* = \mu \left(\frac{(J_{2c}^{xy})^2 - (J_{2,0}^{xy})^2}{(J_{2,0}^{xy})^2} \right)^{\frac{1}{2\epsilon}}$ is the crossover energy scale. It is clear that the power-law vanish of T^* follows:

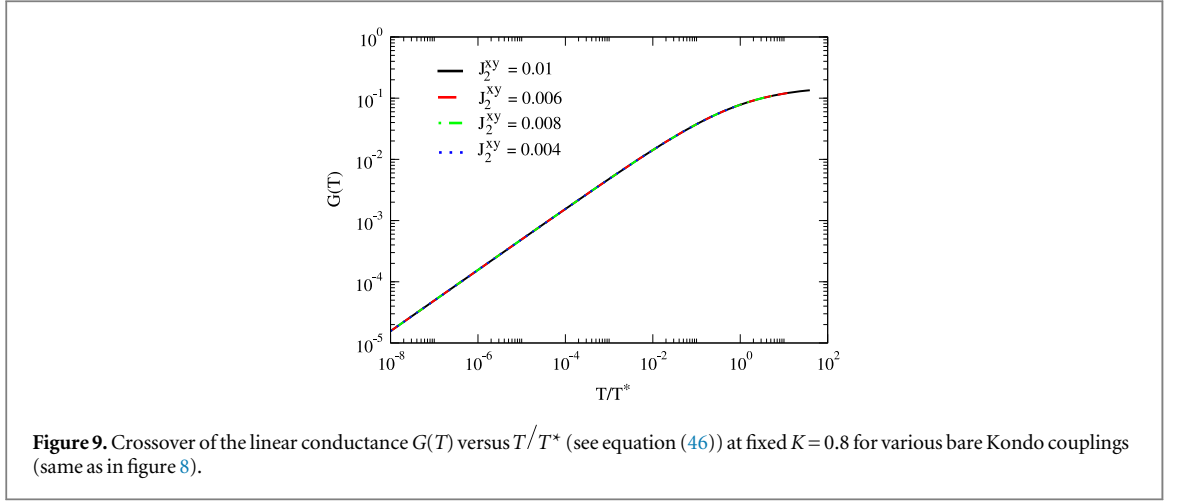
$T^* \propto \mu |t|^{\frac{1}{2\epsilon}} \equiv \mu |t|^\nu$ with the correlation length exponent ν being $\nu = \frac{1}{2\epsilon}$, which agrees with our earlier result in equation (27). The crossover function in equation (42) can be used to compute various crossovers in thermodynamic functions near 1CK-2CK QCP as discussed below.

5.3.1. The impurity susceptibility $T\chi_{\text{imp}}(T)$

The impurity susceptibility is defined as [40, 41]: $\chi_{\text{imp}}(T) = \chi_{\text{imp,imp}} + 2\chi_{u,\text{imp}} + (\chi_{u,u} - \chi_{u,u}^{\text{bulk}})$ where $\chi_{u,u}$ is the bulk response to the local field applied to the bulk only, $\chi_{\text{imp,imp}}$ is the impurity response to the local field applied to the impurity only, $\chi_{u,\text{imp}}$ is the crossed response of the bulk to an impurity field, $\chi_{u,u}^{\text{bulk}}$ is the susceptibility of the bulk in the absence of the impurity. We can calculate $\chi_{\text{imp}}(T)$ via renormalized perturbative approaches in references [40, 41, 45]. We find (up to the first order in j_2^{xy}) $\chi_{\text{imp}}(T)$, contributed from $\chi_{u,\text{imp}}$ (see the Feynmann diagram in figure 3 and equation (24) of reference [45] and equation (9) above), reads:

$$\chi_{u,\text{imp}} = -j_2^{xy} \mu^{-\epsilon} \frac{1}{4T^2} \int_{D_0}^{D_0} d\omega |\omega|^\epsilon \frac{\cosh^{-2}\left(\frac{\omega}{2T}\right)}{4}. \quad (43)$$

Note that the above formula has the same functional form as that shown in equation (24) of reference [45] in the pseudogap Kondo problem at criticality. The exponent r of the pseudogap conduction bath with power-law vanishing density of states (DOS) $\rho(\omega) \propto |\omega|^r$ in reference [45] is now replaced by ϵ in our case as the boson operator $e^{i\sqrt{4\pi\left(\frac{1}{k}-1\right)}\hat{\theta}_a(0)}$ in equation (9) leads to an effective power-law energy dependence ω^ϵ by the Fourier transform in equation (43). Evaluating the above equation in the limit of infinite UV cutoff and up to first order in ϵ , χ_{imp} has the following crossover form (see equation (42) and figure 8):



$$\frac{\chi_{\text{imp}}(T)}{\chi_{\text{imp}}^{\text{2CK}}(T)} \approx 1 - j_2^{xy}(\mu \rightarrow T) \approx 1 - \frac{j_{2c}^{xy}}{\sqrt{1 + \left(\frac{T}{T^*}\right)^{-2\epsilon}}} \quad (44)$$

where $\chi_{\text{imp}}^{\text{2CK}}$ is the impurity susceptibility at the 2CK fixed point, given by [31] $\chi_{\text{imp}}^{\text{2CK}}(T) \propto \frac{\partial C_{\text{imp}}^{\text{2CK}}}{\partial T} \propto \frac{1}{T^{1-\eta_{\chi_{\text{imp}}^{\text{2CK}}}}}$ with impurity specific heat at the 2CK fixed point given by: $C_{\text{imp}}^{\text{2CK}} \propto T^{\frac{2}{K}-2}$ (for $\frac{2}{3} < K < 1$) and $C_{\text{imp}}^{\text{2CK}} \propto T$ (for $K < \frac{2}{3}$) [29, 44]. We have therefore $\eta_{\chi_{\text{imp}}^{\text{2CK}}} = \frac{2}{K} - 2$ (for $\frac{2}{3} < K < 1$) and $\eta_{\chi_{\text{imp}}^{\text{2CK}}} = 1$ (for $K < \frac{2}{3}$).

5.3.2. Impurity entropy $S_{\text{imp}}(T)$

At the 2CK fixed point, the impurity residual entropy has been calculated in [29]: $S_{\text{imp}}^{\text{2CK}} = \ln \sqrt{2K}$. Following [40], the correction to $S_{\text{imp}}^{\text{2CK}}$ near QCP is obtained within the perturbative RG approach by calculating the thermodynamic potential and taking the temperature derivative. The crossover function for the impurity entropy near QCP is found to be (see figure 3 and equation (40) of [40]):

$$\frac{S_{\text{imp}}(T)}{S_{\text{imp}}^{\text{2CK}}} \approx 1 + \frac{\pi^2 \epsilon}{4} \frac{\ln 2}{\ln \sqrt{2K}} \left[j_2^{xy}(\mu \rightarrow T) \right]^2 \approx 1 + \frac{\pi^2 \epsilon}{4} \frac{\ln 2}{\ln \sqrt{2K}} \left[\frac{j_{2c}^{xy}}{\sqrt{1 + \left(\frac{T}{T^*}\right)^{-2\epsilon}}} \right]^2. \quad (45)$$

Note that the prefactor $\frac{1}{4}$ here comes from the j_2^{xy} term only, in contrast to $\frac{3}{8}$ in [40] for the SU(2) symmetric Kondo model.

5.3.3. Equilibrium conductance $G(T)$

The equilibrium conductance $G(T)$ has the following crossover form between the 2CK fixed point and the QCP (see figure 9):

$$G(T) \propto \left[j_2^{xy}(\mu \rightarrow T) \right]^2 \approx \frac{\left[j_{2c}^{xy} \right]^2 T^{2\epsilon}}{T^{2\epsilon} + \left(T^* \right)^{2\epsilon}}. \quad (46)$$

Note that in equilibrium the linear conductance at the 2CK fixed point $G_{\text{2CK}}(T)$ is determined by the bare scaling dimension of the leading irrelevant operator j_2^{xy} , $[j_2^{xy}] = \frac{1}{K}$. This gives $G_{\text{2CK}}(T) \propto T^{2(\frac{1}{K}-1)} = T^{2\epsilon}$. For $T \ll T^*$ where the system reaches the 2CK fixed point, the temperature dependence of $G(T)$ in equation (46) reduces to that at 2CK, $G(T \ll T^*) \propto G_{\text{2CK}}(T)$, as expected.

6. Discussions and conclusions

Before we conclude, we would like to emphasize again the clear physical picture we provided in the introduction to make our main results more transparent. First, it is well known that the stable one-channel and two-channel Kondo fixed points are expected in the case of a Kondo quantum dot coupled to two conventional spinful

Luttinger liquid leads [23, 25]. The ground state of this system changes from 1CK to 2CK when Luttinger parameter K reduces from the non-interacting limit ($K = 1$) to the strongly interacting limit ($K < \frac{1}{2}$). The electron-electron interactions in the Luttinger liquids act equivalently as if an additional dissipative Ohmic boson bath is coupled to the quantum dot [3, 34], leading to suppression in electron transport from one lead to the other through the dot. A quantum phase transition between the 1CK and 2CK fixed points was argued to exist at $K = \frac{1}{2}$ as a direct consequence of the competition between the cross-channel Kondo coupling J_{LR} and the suppression of tunneling due to electron-electron interaction [23, 25]. However, up until now there has been no analytic and controlled approach to access this transition. Note that the one-loop RG approach does not work here to reach to the 1CK-2CK quantum critical point since near the 2CK fixed point the Kondo couplings $J_{LL/RR}$, involved in the renormalization of the cross-channel Kondo coupling J_{LR} , both go to infinity under RG.

When a quantum dot couples to helical Luttinger liquids (a special type of Luttinger liquid), we expect the 1CK and 2CK ground states are also the two possible stable phases for the same reason as mentioned above. However, due to the helical nature of the Luttinger liquid leads, the underlying two-channel Kondo model becomes anisotropic ($J_i^{xy} \neq J_i^z$) as the $SU(2)$ symmetry of the model is broken; while the Kondo model is isotropic ($J_i^{xy} = J_i^z$) for a quantum dot coupled to conventional Luttinger liquid leads. This crucial difference enables us to access the QPT between the 1CK and 2CK fixed points of our system via the controlled RG approach.

In the limit of a weakly interacting helical liquid $K \rightarrow \Gamma$, we find the similar competition between these two possible ground states. The 1CK phase is reached when J_2^{xy} is large enough, while the 2CK phase is reached when the electron-electron interaction becomes strong enough. Via a controlled perturbative RG approach of one-loop order, we find that the 1CK-2CK quantum phase transition occurs near $K = \Gamma$. To reach the 1CK-2CK phase transition in our setup, we believe it is necessary to go beyond the tree-level bare scaling dimension analysis, which predicts a stable 2CK phase for as long as $K < 1$ [29]. The one-loop RG is the leading correction to the above-mentioned bare scaling dimension analysis. Note that the main difference between the case for conventional Luttinger liquid and that for helical liquid is that the resulting two-channel Kondo model is isotropic in the former case, while it is anisotropic in the latter case. This difference affects details of the critical properties, such as the critical points occurring at $K = K_c = \frac{1}{2}$ for the Kondo dot coupled to Luttinger liquid, while we find the existence of $K_c < 1$ by the RG analysis near the strong coupling 2CK fixed point for the case of helical Luttinger liquid. At a general level, however, we should expect a 1CK-2CK quantum phase transition to exist in both cases.

Meanwhile, within our one-loop RG analysis, the two Kondo couplings j_2^{xy} and δj_1^z terms scale with different powers of ϵ at critical point. Therefore, the loop orders in general can mix (i.e. the two-loop results for critical Kondo couplings may lead to the same order in ϵ as that at one-loop order). To estimate the corrections at higher loop orders to our results at one-loop order, we include the two-loop order terms $\frac{1}{4}(j_2^{xy})^3$ and $\frac{1}{2}(j_2^{xy})^2 j_2^z$ in RG scaling equations for j_2^{xy} and δj_1^z terms in equation (19), respectively [39]. We find that this modification will lead to a small correction (shift) to the locations of the critical Kondo couplings: $(\delta j_{1,c}^z, j_{2,c}^{xy}) \rightarrow (a\epsilon, b\sqrt{\epsilon\epsilon'})$ with $a = \frac{1}{1-\epsilon'/4} \approx \frac{8}{7}$, $b = \frac{1}{\sqrt{1-\epsilon'/4}} \approx \sqrt{\frac{8}{7}}$. Therefore, this correction will not spoil our main results as it only slightly modifies the critical exponents of observables for those depending on the location of the critical Kondo couplings.

In summary, we have re-examined [29] on the two-channel Kondo physics in the Kondo quantum dot coupled to two helical edge states of two-dimensional topological insulators. Via the one-loop renormalization group approach which goes beyond the scaling dimension analysis in [29], we found the quantum phase transition between the one-channel (1CK) and two-channel (2CK) Kondo ground states for weakly interacting leads ($K \rightarrow \Gamma$). We made definite predictions on the critical properties when the system is close to the transition. Our results are robust for $\frac{1}{2} < K < 1$, and they refine the statement in [29] that the two-channel Kondo ground state is stable for as long as $K < 1$. Our results also provide the first theoretical realization of the quantum phase transition between 1CK and 2CK physics in Kondo impurity models. Further investigations via field-theoretical and numerical renormalization group (NRG) [12] approaches are needed in order to clarify the critical properties, including the critical exponents and finite-temperature dynamics in crossover functions associated with the transition [45]. Our results motivates the search for these critical properties near the 1CK-2CK quantum phase transition in future experiments on a Kondo quantum dot coupled to 2D topological insulators.

Acknowledgments

We thank M Vojta, T K Ng, K T Law, Y W Li and H H Lin for helpful discussions, and T H Lee for technical support. This work is supported by the NSC grant no. 98-2918-I-009-06, no. 98-2112-M-009-010-MY3, the NCTU-CTS, the MOE-ATU program, and the NCTS of Taiwan, Republic of China.

Appendix A. The RG scaling equation in the weak-coupling regime via bosonization

In this appendix, we provide some details on deriving the RG scaling equations of equation (3) for $K \rightarrow 1^-$ from the bosonized Hamiltonian equation (2). Following [33] and [31], we decompose the boson fields $\Phi_\nu \equiv \theta_\nu, \phi_\nu$ with $\nu = s, a$ into the ‘fast’ ($\Phi_\nu^>$) and ‘slow’ ($\Phi_\nu^<$) components:

$$\begin{aligned}\Phi_\nu(\tau) &= \Phi_\nu^<(\tau) + \Phi_\nu^>(\tau), \\ \Phi_\nu^<(\tau) &= \frac{1}{\beta} \sum_{|\omega_n| < \mu'} \Phi(\omega_n), \\ \Phi_\nu^>(\tau) &= \frac{1}{\beta} \sum_{\mu' < |\omega_n| < \mu} \Phi(\omega_n)\end{aligned}\quad (\text{A.1})$$

with $\mu' = \mu + d\mu$. The partition function can be decomposed in the following form:

$$\begin{aligned}Z_\mu &= \int D\Phi^< D\Phi^> e^{-S_0[\Phi^<] - S_0[\Phi^>] - S_{\text{int}}[\Phi^< + \Phi^>]}, \\ &= Z_0 \int D\Phi^< e^{-S_0[\Phi^<]} \left\langle e^{-S_{\text{int}}[\Phi^< + \Phi^>]} \right\rangle_f\end{aligned}\quad (\text{A.2})$$

where

$$\begin{aligned}Z_0 &\equiv \int D\Phi^> e^{-S_0[\Phi^>]}, \\ \langle \mathcal{A} \rangle_f &\equiv \int D\Phi^> e^{-S_0[\Phi^>]} \mathcal{A}[\Phi^>].\end{aligned}\quad (\text{A.3})$$

The partition function Z_μ can be re-expressed by exponentiating $\langle \dots \rangle_f$ in the integrand in terms of the effective action $S_{\text{eff}}[\Phi^<] \equiv \int d\tau \mathcal{L}_K(\Phi^<)$ with \mathcal{L}_K being the Lagrangian of the Kondo model (see equation (2)), involving only the slow component of the fields with the following form via the cumulant expansion:

$$\begin{aligned}S_{\text{eff}}[\Phi^<] &= S_0[\Phi^<] - \ln \left\langle e^{-S_{\text{int}}[\Phi^< + \Phi^>]} \right\rangle, \\ &= S_0[\Phi^<] + \left\langle S_{\text{int}}[\Phi^< + \Phi^>] \right\rangle_f \\ &\quad - \frac{1}{2} \left(\left\langle S_{\text{int}}^2[\Phi^< + \Phi^>] \right\rangle - \left\langle S_{\text{int}}[\Phi^< + \Phi^>] \right\rangle_f^2 \right) + \dots\end{aligned}\quad (\text{A.4})$$

The RG procedure is carried out by integrating out the fast modes of bosons and expressing the effective low-energy theory in the original form with the renormalized couplings. The following two-point correlation functions of boson fields prove to be useful in the RG analysis [33]:

$$\begin{aligned}G(x, \tau) &= \langle \Phi(x, \tau) \Phi(0, 0) \rangle_f = \int \frac{dk}{2\pi} \int \frac{d\omega}{2\pi} e^{-ikx} e^{i\omega\tau} \frac{\pi}{\frac{\omega^2}{v_F^2} + v_F' k^2}, \\ G(\tau) \equiv G(0, \tau) &= \begin{cases} \frac{1}{2\pi} K_0(\mu'\tau) & \text{for } \mu'\tau \gg 1 \\ \frac{1}{2\pi} \ln \frac{\mu}{\mu'} & \text{for } \mu'\tau \ll 1, \end{cases}\end{aligned}\quad (\text{A.5})$$

where K_0 is the Bessel function of the second kind. It is clear from equation (A.5) that $G(\tau)$ can be considered a short-ranged function of τ .

First, we focus on the first order cumulant $\langle S_{\text{int}}[\Phi^> + \Phi^<] \rangle$, which leads to the bare scaling dimensions of various Kondo couplings in [29]. The renormalization of the forward longitudinal term J_1^z term, δJ_1^z , gives:

$$J_1^z \int d\tau \langle \partial_x \theta_s(0, \tau) \rangle_f = J_1^z \int d\tau \left[\langle \partial_x \theta_s^<(0, \tau) \rangle + \langle \partial_x \theta_s^>(0, \tau) \rangle_f \right]. \quad (\text{A.6})$$

Since θ_s is an odd function in spin space, its average vanishes, $\langle \partial_x \theta_s^>(0, \tau) \rangle_f = 0$, $\delta J_1^z = 0$. This gives the first-order RG scaling equation:

$$\frac{dj_1^z}{d \ln \mu} = 0 \quad (\text{A.7})$$

with the renormalized dimensionless coupling j_1^z defined as: $j_1^z = \rho_0 J_1^z$ where $\rho_0 = \frac{1}{\pi v_f}$ is the density of states. The rescaling of the backward longitudinal term J_2^z term leads to:

$$\begin{aligned} \int d\tau J_2^z \left\langle \sin \left(\sqrt{\frac{2\pi}{K}} \theta_a(0, \tau) \right) \right\rangle_f \left\langle \sin \left(\sqrt{2\pi K} \phi_a(0, \tau) \right) \right\rangle_f &= \left(\frac{\mu'}{\mu} \right)^{\frac{K}{2} + \frac{1}{2K}} \\ \times \int d\tau J_2^z \sin \left(\sqrt{\frac{2\pi}{K}} \theta_s^<(0, \tau) \right) \sin \left(\sqrt{2\pi K} \phi_s^<(0, \tau) \right) & \quad (\text{A.8}) \end{aligned}$$

where equation (A.5) and $\langle e^A \rangle = e^{\frac{1}{2}\langle A^2 \rangle}$ are used [31]. This relation is justified for any operator A that is linear in terms of boson fields whose Hamiltonian is quadratic in those boson fields, which is precisely the case for the A operator we apply here. Upon rescaling $\tau, \tau \rightarrow \tau \frac{\mu}{\mu'}$, we may define the new dimensionless renormalized coupling $j_2^z(\mu)$ in terms of the bare coupling $J_2^z(\mu = \mu_0 = 1)$ as:

$$j_2^z(\mu) = \rho_0 \mu^{\frac{K}{2} + \frac{1}{2K} - 1} J_2^z, \quad (\text{A.9})$$

we arrive at the RG scaling equation at the level of bare scaling dimension:

$$\frac{dj_2^z}{d \ln \mu} = \left(\frac{K + 1/K}{2} - 1 \right) j_2^z. \quad (\text{A.10})$$

The first-order RG scaling equations for the remaining couplings are obtained similarly:

$$\frac{dj_1^{xy}}{d \ln \mu} = (K - 1) j_1^{xy}, \quad \frac{dj_2^{xy}}{d \ln \mu} = \left(\frac{K + 1/K}{2} - 1 \right) j_2^{xy} \quad (\text{A.11})$$

with the renormalized dimensionless couplings defined in the text.

Next, we consider the second order cummulant terms generated from $-\frac{1}{2}(\langle S_{\text{int}}^2[\Phi^< + \Phi^>] \rangle - \langle S_{\text{int}}[\Phi^< + \Phi^>] \rangle_f^2)$. In general, the second-order contributions to the renormalization of various couplings have the following form:

$$\begin{aligned} \frac{dj_1^{xy}}{d \ln \mu} &= -a_1 j_1^{xy} j_1^z - a_2 j_2^{xy} j_2^z, \quad \frac{dj_1^z}{d \ln \mu} = -b_1 (j_1^{xy})^2 - b_2 (j_2^{xy})^2, \\ \frac{dj_2^{xy}}{d \ln \mu} &= -c_1 j_1^{xy} j_2^z - c_2 j_2^{xy} j_1^z, \quad \frac{dj_2^z}{d \ln \mu} = -2d_1 j_1^{xy} j_2^{xy}, \end{aligned} \quad (\text{A.12})$$

with a_i, b_i, c_i , and d_i being the pre-factors to be determined.

We first focus on the terms in $J_2^{xy} J_2^z$ which will contribute to the renormalization of j_1^{xy} :

$$\begin{aligned} \frac{2J_2^{xy} J_2^z}{(\pi a)^2} S_2 S^+ \int d\tau \int d\tau' & \\ \times 2 \left[\left\langle e^{-i\sqrt{2\pi K} \phi_s(0, \tau)} \cos \left(\sqrt{\frac{2\pi}{K}} \theta_a(0, \tau) \right) \right. \right. & \\ \times \sin \left(\sqrt{\frac{2\pi}{K}} \theta_a(0, \tau') \right) \sin \left(\sqrt{2\pi K} \phi_a(0, \tau') \right) \Big\rangle_f & \\ - \left\langle e^{-i\sqrt{2\pi K} \phi_s(0, \tau)} \cos \left(\sqrt{\frac{2\pi}{K}} \theta_a(0, \tau) \right) \right\rangle_f & \\ \times \left. \left\langle \sin \left(\sqrt{\frac{2\pi}{K}} \theta_a(0, \tau') \right) \sin \left(\sqrt{2\pi K} \phi_a(0, \tau') \right) \right\rangle_f \right] & \quad (\text{A.13}) \end{aligned}$$

After averaging over the fast modes and rescaling τ , τ' , we arrive at:

$$\begin{aligned} & \frac{J_2^{xy} J_2^z}{(\pi a)^2} S^+ \int d\tau \int d\tau' \left(\frac{\mu'}{\mu} \right)^{\frac{1}{K} + K - 2} \\ & \times \left[\left(\frac{\mu'}{\mu} \right)^{\frac{-1}{K}} - 1 \right] e^{-i\sqrt{2\pi K} \phi_s^<(0, \tau)} \cos \left(\sqrt{2\pi K} \phi_a^<(0, \tau') \right). \end{aligned} \quad (\text{A.14})$$

In deriving the above equation, we have decomposed the terms $\sin(\sqrt{2\pi K} \phi_a(\tau'))$ and $\cos(\sqrt{\frac{2\pi}{K}}(\theta_a(\tau)) \sin(\sqrt{\frac{2\pi}{K}}(\theta_a(\tau'))$ into the fast and the slow modes, and kept only the leading (more relevant) terms. In the limit of $\tau, \tau' \ll \frac{1}{\mu} \approx a$, we may get rid off one of the double time-integrals in the above equation by introducing a short-time cutoff $\tau_0 \approx \frac{a}{v_F}$. The logarithmic correction of equation (A.14) is obtained by expanding $(\frac{\mu'}{\mu})^{\frac{-1}{K}} - 1$ to the leading order: $(\frac{\mu'}{\mu})^{\frac{-1}{K}} - 1 \approx -\frac{1}{K} \frac{d\mu}{\mu} + g(\mu)$ where $g(\mu)$ contains sub-leading (less singular) terms of μ which we neglect here at one-loop RG. In the limit of $K \rightarrow \Gamma$, equation (A.14) becomes:

$$-\frac{J_2^{xy} J_2^z}{\pi a} S^+ \int d\tau \frac{d\mu}{\mu} e^{-i\sqrt{2\pi K} \phi_s^<(0, \tau)} \cos \left(\sqrt{2\pi K} \phi_a^<(0, \tau) \right). \quad (\text{A.15})$$

Therefore, the pre-factor a_2 in equation (A.12) is found to be $a_2 = 1$. Similarly, we find the pre-factors $c_1 = b_1 = b_2 = d_1 = 1$ in equation (A.12).

Next, we consider a different type of renormalization involving J_1^z terms. We may focus on a typical term $J_1^{xy} J_1^z$, which renormalizes J_1^{xy} :

$$\begin{aligned} & -a \sqrt{\frac{2\pi}{K}} \frac{J_1^{xy} J_1^z}{(\pi a)^2} \int d\tau \int d\tau' S^- S_z \\ & \times \left[\langle \partial_x \theta_s(0, \tau) \right. \\ & \times e^{-i\sqrt{2\pi K} \phi_s(0, \tau')} \cos(\sqrt{2\pi K} \phi_a(0, \tau')) \Big\rangle_f \\ & - \langle \partial_x \theta_s(0, \tau) \rangle_f \\ & \times \left. \left\langle d^{-i\sqrt{2\pi K} \phi_s(0, \tau')} \cos(\sqrt{2\pi K} \phi_a(0, \tau')) \right\rangle_f \right] \\ & = -a \sqrt{\frac{2\pi}{K}} \frac{J_1^{xy} J_1^z}{(\pi a)^2} \int d\tau \int d\tau' S^- S_z \\ & \times \left[\langle \partial_x \theta_s^>(0, \tau) \right. \\ & \times e^{-i\sqrt{2\pi K} \phi_s(0, \tau')} \cos(\sqrt{2\pi K} \phi_a(0, \tau')) \Big\rangle_f \Big]. \end{aligned} \quad (\text{A.16})$$

We may use the following identities [33] to simplify equation (A.16):

$$\begin{aligned} & \left\langle \partial_x \sqrt{\frac{2\pi}{K}} \theta_s^>(0, \tau) e^{-i(\sqrt{2\pi K} \phi_s(0, \tau'))} e^{i\sqrt{2\pi K} \phi_a(0, \tau')} \right\rangle_f \\ & \lim_{\eta \rightarrow 0} \frac{1}{i\eta} \partial_x \left\langle e^{i\eta \sqrt{\frac{2\pi}{K}} \theta_s^>(x, \tau)} e^{-i\sqrt{2\pi K} \phi_s^>(0, \tau')} e^{i\sqrt{2\pi K} \phi_a^>(0, \tau')} \right\rangle_f \Big|_{x=0} \\ & \times e^{-i(\sqrt{2\pi K} \phi_s^<(0, \tau'))} e^{i\sqrt{2\pi K} \phi_a^<(0, \tau')}, \end{aligned} \quad (\text{A.17})$$

and

$$e^{A+B} = e^A e^B e^{\frac{1}{2}[A, B]}. \quad (\text{A.18})$$

With the above relations, equation (A.17) becomes:

$$\begin{aligned}
& \lim_{\eta \rightarrow 0} \frac{1}{i\eta} \partial_x \left\langle e^{i\sqrt{2\pi} \left(\eta \sqrt{\frac{1}{K}} \theta_s^>(x, \tau) - \sqrt{K} \phi_s^>(0, \tau') \right)} \right\rangle_f \Big|_{x=0} \\
& \quad \times \left\langle e^{i\sqrt{2\pi K} \phi_a^>(0, \tau')} \right\rangle_f \\
& \quad \times e^{-i\sqrt{2\pi K} \phi_s^<(0, \tau')} e^{i\sqrt{2\pi K} \phi_a^<(0, \tau')}, \\
& = \frac{1}{i} \left(\frac{\pi}{K} \partial_x G_{\theta_s^>(x, \tau)} + 2\pi \partial_x \langle \theta_s^>(x, \tau) \phi_s^>(0, \tau') \rangle_f \right) \Big|_{x=0} \\
& \quad \times \left\langle e^{i\sqrt{2\pi K} \phi_s^>(0, \tau')} \right\rangle_f < e^{i\sqrt{2\pi K} \phi_a^>(0, \tau')} \Big|_f \\
& \quad \times e^{-i(\sqrt{2\pi K} \phi_s^<(0, \tau'))} e^{i\sqrt{2\pi K} \phi_a^<(0, \tau')}. \tag{A.19}
\end{aligned}$$

The leading logarithmic correction comes from the term $\partial_x \langle \theta_s^>(x, \tau) \phi_s^>(0, \tau') \rangle_f$, which can be evaluated via the following relations [33]:

$$-\frac{i}{v_F'} \frac{\partial \phi_s}{\partial \tau} = \frac{\partial \theta_s}{\partial x}, \quad -\frac{i}{v_F'} \frac{\partial \theta_s}{\partial \tau} = \frac{\partial \phi_s}{\partial x}. \tag{A.20}$$

We have therefore

$$\partial_x \langle \theta_s^>(x, \tau) \phi_s^>(0, \tau') \rangle_f = \frac{-i}{v_F'} \frac{\partial}{\partial \tau} < \theta_s^>(x, \tau) \theta_s^>(0, \tau') \rangle_f. \tag{A.21}$$

After collecting all the terms and performing re-scaling, equation (A.16) becomes:

$$\begin{aligned}
& -\frac{1}{\pi v_F'} \frac{J_1^{xy} J_1^z}{\pi a} \int d\tau S^{-} \left(\frac{\mu'}{\mu} \right)^{K-1} \frac{d\mu}{\mu} \\
& \quad \times e^{-i(\sqrt{2\pi K} \phi_s^<(0, \tau'))} \cos \left(\sqrt{2\pi K} \phi_a^<(0, \tau') \right). \tag{A.22}
\end{aligned}$$

Finally, the correction to j_1^{xy} contributed from $J_1^{xy} J_1^z, \delta j_{1, j_1^{xy} j_1^z}^{xy}$, reads:

$$\begin{aligned}
\delta j_{1, j_1^{xy} j_1^z}^{xy} & = -j_1^{xy} j_1^z \frac{d\mu}{\mu} \int d\tau e^{-i\sqrt{2\pi K} \phi_s^<(0, \tau)} \\
& \quad \times \cos \left(\sqrt{2\pi K} \phi_a^<(0, \tau) \right), \tag{A.23}
\end{aligned}$$

where $j_1^{xy} \equiv \rho_0 \mu^{K-1} J_1^{xy}, j_1^z \equiv \frac{\rho_0}{\pi v_F'} J_1^z$. We therefore find $a_1 = 1$. Similarly, we find $c_2 = 1$. Combining the first and second order corrections to the renormalization of various Kondo couplings, equation (3) follows.

Appendix B. The one-loop RG scaling equations near the 2CK fixed point via poor-man's scaling

In this appendix, we derive the RG equations in equation (19) from the effective Kondo Hamiltonian equation (9) via poor-man's scaling, as shown in [34]. Based on the scaling dimensions of various Kondo couplings in the strong coupling 2CK regime, we take the logarithmic derivative of the proposed new dimensionless Kondo couplings $j_2^{xy} \equiv \rho_0 \tilde{c}_2^\perp \mu^\epsilon J_2^{xy}, \delta j_1^z \equiv \rho_0 \tilde{c}_1^z \mu^{\epsilon'} \frac{\pi}{\sqrt{K}} \delta J_1^z$ (see text) with respect to the cutoff energy μ .

First, we focus on the RG equation for j_2^{xy} :

$$\frac{\partial j_2^{xy}}{\partial \ln \mu} = \epsilon j_2^{xy} - \mu^\epsilon \rho_0 \tilde{c}_2^\perp \frac{\partial J_2^{xy}}{\partial \ln \mu}. \tag{B.1}$$

The derivative of J_2^{xy} w.r.t. $\ln \mu$ is given by:

$$\frac{\partial J_2^{xy}}{\partial \ln \mu} = \frac{\partial}{\partial \ln \mu} \int_{\mu_0}^{\mu} d\omega \left[J_2^{xy} \delta J_1^z \frac{\rho_{2xy, 1z}(\omega)}{-\omega} \right]. \tag{B.2}$$

Here, $\rho_{2xy, 1z}(\omega)$ is the effective electron density of states due to the additional phase correlations associated with the product of J_2^{xy} and δJ_1^z terms in equation (9). Following [34], this is equivalent to replacing the free electron Green's function of the effective leads: $G_{\alpha, 0}^\sigma(t) \equiv \langle \tilde{c}_\alpha^\dagger(t) \tilde{c}_\alpha^\sigma(0) \rangle$ by a 'mixed' one:

$$\begin{aligned}\tilde{G}_L^{\uparrow(4)}(t) &\equiv \left\langle \tilde{c}_L^{\uparrow(4)}(t) \tilde{c}_L^{\uparrow(4)}(0) \times e^{\pm i \sqrt{4\pi \left(\frac{1}{K}-1\right)} \tilde{\theta}_a(t)} S^\pm(0) S_z(t) \right\rangle \\ &\approx G_{L,0}^{\uparrow(4)}(t) \times \left\langle e^{\pm i \sqrt{4\pi \left(\frac{1}{K}-1\right)} \tilde{\theta}_a(t)} \right\rangle \langle S^\pm(0) S_z(t) \rangle.\end{aligned}\quad (\text{B.3})$$

($\tilde{G}_R^\sigma(t)$ can be defined similarly.) Therefore, $\rho_{2xy,1z}(\omega) \equiv \frac{-1}{\pi} \sum_\sigma \text{Im}(\tilde{G}_\alpha^\sigma(\omega))$ reads [34]:

$$\begin{aligned}\rho_{2xy,1z}(\omega) &= \rho_0 \int_0^\omega dE P_{2\perp 1z}(E), \\ P_{2\perp 1z}(E) &= \frac{1}{2\pi} \int dt \langle \hat{O}_{2\perp 1z}(t) \rangle e^{iEt}\end{aligned}\quad (\text{B.4})$$

where $\rho_0 = \frac{-1}{\pi} \sum_\sigma \text{Im}(G_{\alpha,0}^\sigma(\omega))$ is the constant density of states of the non-interacting leads, and $\langle \hat{O}_{2\perp 1z}(t) \rangle$ has the following typical form:

$$\langle \hat{O}_{2\perp 1z}(t) \rangle = \left\langle e^{\pm i \sqrt{4\pi \left(\frac{1}{K}-1\right)} \tilde{\theta}_a(t)} \right\rangle \langle S^\pm(0) S_z(t) \rangle.\quad (\text{B.5})$$

Since the exponential factors in $\hat{O}_{2\perp 1z}(t)$ are unpaired, it gives a trivial result: $\langle e^{\pm i \sqrt{4\pi \left(\frac{1}{K}-1\right)} \tilde{\theta}_a(t)} \rangle = 1$, and hence it does not affect the renormalization of the couplings [34]. Nevertheless, $\langle S^\pm(0) S_z(t) \rangle$ shows non-trivial correlations [29]:

$$\langle S^\pm(0) S_z(t) \rangle \approx \frac{1}{(i\omega_c t)^{\epsilon'}}\quad (\text{B.6})$$

with ω_c being a high-energy cutoff. We have therefore

$$\begin{aligned}\rho_{2xy,1z}(\omega) &= \rho_0 \int_0^\omega dE P_{2\perp 1z}(E) = \rho_0 \tilde{c}_2 \omega^{2\epsilon'}, \\ P_{2\perp 1z}(E) &= \frac{1}{2\pi} \int dt \langle \hat{O}_{2\perp 1z}(t) \rangle e^{iEt} = \tilde{c}_2^\perp E^{\epsilon'-1}\end{aligned}\quad (\text{B.7})$$

with $\tilde{c}_2 = A(\epsilon') = \frac{1}{\pi\omega_c^{\epsilon'}} \sin(\pi\epsilon') \Gamma(1+\epsilon')$ with $\epsilon' = \frac{1}{2K}$ and Γ being the Gamma function.

The integral in equation (B.2) gives:

$$\begin{aligned}\rho_0^2 \tilde{c}_2^\perp \mu^\epsilon J_2^{xy} \delta J_1^z \int_{\mu_0}^\mu d\omega \frac{\rho_{2xy,1z}(\omega)}{-\omega} \\ = -\rho_0^2 \tilde{c}_2^\perp A(\epsilon') \mu^\epsilon \mu^{\epsilon'} J_2^{xy} \delta J_1^z \ln \frac{\mu}{\mu_0}.\end{aligned}\quad (\text{B.8})$$

Similarly, we find the RG scaling equation for δj_1^z is given by:

$$\frac{\partial \delta j_1^z}{\partial \ln \mu} = \epsilon' \delta j_1^z - \rho_0^2 \tilde{c}_1^z A(2\epsilon) \mu^{2\epsilon} (J_2^{xy})^2\quad (\text{B.9})$$

where the effective density of states is used [34]:

$$\begin{aligned}\rho_{2\perp,2\perp}(\omega) &= \rho_0 \int_0^\omega dE P_{2\perp 2\perp}(E), \\ P_{2\perp 2\perp}(E) &= \int dt \langle \hat{A}(t) \rangle e^{iEt}, \\ \langle \hat{A}(t) \rangle &= \left\langle e^{-i \sqrt{4\pi \left(\frac{1}{K}-1\right)} \tilde{\theta}_a(t)} e^{i \sqrt{4\pi \left(\frac{1}{K}-1\right)} \tilde{\theta}_a(0)} \right\rangle \\ &\approx \frac{1}{(i\omega_c t)^{2\epsilon}}.\end{aligned}\quad (\text{B.10})$$

We may determine the pre-factors \tilde{c}_2^\perp , \tilde{c}^z by the following identifications: $\tilde{c}_2^\perp = \sqrt{A(\epsilon')A(\epsilon')}$, $\tilde{c}_1^z = A(\epsilon')$. With the above results, we finally arrive at the RG scaling equations shown in equation (19).

Appendix C. The one-loop RG equations near the 2CK fixed point via the ϵ -expansion technique

In this appendix, we offer an alternative route to equation (19) via the ϵ -expansion technique [37–41].

We first derive the renormalization factors $Z_{j^\perp/z}$ and Z_f shown in equation (26). We focus on the one-loop renormalization of the dimensionless couplings $\tilde{J}_2^{xy} \equiv \rho_0 \tilde{c}_2^\perp \mu^\epsilon J_2^{xy}$, and $\delta J_1^z \equiv \rho_0 \tilde{c}_1^z \mu^{\epsilon'} \sqrt{\frac{\pi}{K}} \delta J_1^z$. Let us look at vertex renormalization of \tilde{J}_1^z , defined as the dimensionless renormalized coupling δj_1^z , first [39, 40]:

$$\delta j_1^z \equiv Z_{j^z}^{-1} \delta \tilde{J}_1^z = \delta \tilde{J}_1^z \left[1 + \frac{(J_2^{xy})^2}{\delta \tilde{J}_1^z} \int^\mu d\omega \frac{\rho_\perp(\omega)}{-\omega} \right] \quad (\text{C.1})$$

where the effective density of states reads [34]:

$$\begin{aligned} \rho_\perp(\omega) &= \rho_0 \int_0^\omega dE P_\perp(E), \quad P_\perp(E) = \int dt \langle \hat{A}(t) \rangle e^{iEt}, \\ \langle \hat{A}(t) \rangle &= \left\langle e^{-i\sqrt{4\pi}\hat{\theta}_a(t)} e^{i\sqrt{4\pi}\hat{\theta}_a(0)} \right\rangle \approx \frac{1}{(i\omega_c t)^{2\epsilon}}. \end{aligned} \quad (\text{C.2})$$

From above, we find $P_\perp(E) = \tilde{c}_1 E^{2\epsilon-1}$ with $\tilde{c}_1 = A(2\epsilon)$ and the constant $A(\epsilon)$ being defined in appendix B.

Therefore, we have

$$\rho_\perp(\omega) = \rho_0 \tilde{c}_1 \omega^{2\epsilon}. \quad (\text{C.3})$$

Plugging these results into equation (C.1) and via the proper identification: $\tilde{c}_2^\perp \equiv \sqrt{\tilde{c}_1} = \sqrt{A(2\epsilon)}$, at the leading order in $(j_2^{xy})^2 / \delta j_1^z$, Z_{j^z} reads:

$$Z_{j^z} = 1 + \frac{(j_2^{xy})^2 / \delta j_1^z}{2\epsilon}. \quad (\text{C.4})$$

Similarly, we can show that

$$Z_{j^\perp} = 1 + \frac{j_1^z}{\epsilon'} \quad (\text{C.5})$$

where the following relations are used:

$$\begin{aligned} \rho_z(\omega) &= \frac{\rho_0}{2\pi} \int_0^\omega dE P_z(E) = \rho_0 \tilde{c}_2 \omega^{2\epsilon'}, \\ P_z(E) &= \int dt \langle \hat{B}(t) \rangle e^{iEt} = \tilde{c}_2 E^{\epsilon'-1}, \\ \hat{B}(t) &\equiv \langle S^\pm(0) S_z(t) \rangle \approx \frac{1}{(i\omega_c t)^{\epsilon'}} \end{aligned} \quad (\text{C.6})$$

with $\tilde{c}_2 = A(\epsilon')$, and $\tilde{c}_1^z = \sqrt{\tilde{c}_1} / \tilde{c}_2$.

Next, we provide the derivation for Z_f . Following [39], the self energy at one-loop order (see figure 5(a) of [39]) leads to the following renormalization factor Z_f for the impurity fermion:

$$Z_f = 1 + \frac{(J_2^{xy})^2}{4} \int^\mu d\omega \frac{\rho_\perp(\omega)}{\omega} + \frac{(\delta J_1^z)^2}{8} \int^\mu d\omega \frac{\rho_z(\omega)}{\omega}. \quad (\text{C.7})$$

Plugging equations (C.3) and (C.6) into equation (C.7) and expressing the results in terms of the dimensionless renormalized couplings \tilde{j}_2^{xy} and δj_1^z , we arrive at:

$$Z_f = 1 + \frac{(\tilde{j}_2^{xy})^2}{8\epsilon} + \frac{(\delta j_1^z)^2}{16\epsilon'}. \quad (\text{C.8})$$

With Z_β , Z_{j^\perp} , Z_{j^z} to hand, we now can reproduce the RG scaling equations, equation (19), via the β -function within the field-theoretical ϵ -expansion approach:

$$\beta(\delta j_1^z) \equiv \mu \frac{\partial \delta j_1^z}{\partial \mu} \Big|_{J_2^{xy}, \delta J_1^z}, \quad \beta(j_2^{xy}) \equiv \mu \frac{\partial j_2^{xy}}{\partial \mu} \Big|_{J_2^{xy}, \delta J_1^z} \quad (\text{C.9})$$

with the relations between the bare Kondo couplings δJ_1^z , J_2^{xy} and the renormalized ones δj_1^z , \tilde{j}_2^{xy} being

$$J_2^{xy} = \frac{\mu^{-\epsilon} Z_{j^\perp}}{Z_f} \tilde{j}_2^{xy}, \quad \text{and} \quad \delta J_1^z = \frac{\mu^{-\epsilon'} Z_{j^z} \sqrt{K}}{Z_f \pi} \delta j_1^z.$$

Appendix D. The RG scaling equations in the strong-coupling 2CK limit via bosonization

In this appendix, we offer an alternative route to the RG scaling equations, equation (19), at the 2CK fixed point via bosonization. The Hamiltonian at 2CK equation (5) can be expressed more rigorously by including the Klein factors [34], which proves to be important in deriving the RG scaling equation:

$$\begin{aligned} \delta H_{2\text{CK}} = & \frac{J_2^{xy}}{2\pi a} S^+ F_s \left[F_f e^{i\sqrt{\frac{2\pi}{K}} \theta_a(0)} + F_f^\dagger e^{-i\sqrt{\frac{2\pi}{K}} \theta_a(0)} \right] + \text{h.c.} \\ & - \sqrt{\frac{2\pi}{K}} \delta J_1^z S_z \partial_x \theta_s(0). \end{aligned} \quad (\text{D.1})$$

where F_s , F_f , F_{sf} are Klein factors satisfying the following relations [34]:

$$\begin{aligned} F_s F_f &= F_2^{\dagger\downarrow} F_1^\uparrow, \\ F_s F_f^\dagger &= F_1^{\dagger\downarrow} F_2^\uparrow, \\ F_{sf} F_s^\dagger &= F_2^{\dagger\uparrow} F_2^\downarrow, \\ F_{sf}^\dagger F_f^\dagger &= F_1^{\dagger\uparrow} F_2^\uparrow. \end{aligned} \quad (\text{D.2})$$

Following the approach in appendix A, we first focus on the term $J_2^{xy} \delta J_1^z$, which will contribute to the renormalization of J_2^{xy} . One of its contributions is given by:

$$\begin{aligned} \delta j_2^{xy} \propto & - \sqrt{\frac{2\pi}{K}} \frac{J_2^{xy} \delta J_1^z}{2\pi a} F_s F_f \int d\tau \int d\tau' S^+(\tau') S_z(\tau) \\ & \times \left[\left\langle \partial_x \theta_s(0, \tau) e^{i\sqrt{\frac{2\pi}{K}} \theta_a(0, \tau')} \right\rangle_f \right. \\ & \left. - \langle \partial_x \theta_s(0, \tau) \rangle_f \left\langle e^{i\sqrt{\frac{2\pi}{K}} \theta_a(0, \tau')} \right\rangle_f \right] \\ = & - \sqrt{\frac{2\pi}{K}} \frac{J_2^{xy} \delta J_1^z}{2\pi a} F_s F_f \int d\tau \int d\tau' S^+(\tau') S_z(\tau) \\ & \times \left\langle \partial_x \theta_s^>(0, \tau) e^{i\sqrt{\frac{2\pi}{K}} \theta_a(0, \tau')} \right\rangle_f. \end{aligned} \quad (\text{D.3})$$

Following similar steps to those shown in equation (A.17), we may rewrite equation (D.3) as:

$$\begin{aligned} \delta j_2^{xy} \propto & - \frac{J_2^{xy} \delta J_1^z}{2\pi a} F_s F_f \int d\tau \int d\tau' S^+(\tau') S_z(\tau) \\ & \times \left[\lim_{\eta \rightarrow 0} \frac{1}{i\eta} \partial_x \left\langle e^{i\eta \sqrt{\frac{2\pi}{K}} \theta_s^>(x, \tau)} e^{-i\sqrt{2\pi K} \phi_s^>(x', \tau')} \right. \right. \\ & \times \left. \left. e^{i\sqrt{2\pi K} \phi_s^>(x', \tau')} \right\rangle_f \Big|_{x, x' \rightarrow 0} \right. \\ & \times e^{-i\sqrt{2\pi K} \phi_s^<(x', \tau')} e^{i(\sqrt{2\pi K} \phi_s^<(x', \tau'))} \\ & \left. \times \left\langle e^{i\sqrt{\frac{2\pi}{K}} \theta_a^>(0, \tau')} \right\rangle_f e^{i\sqrt{\frac{2\pi}{K}} \theta_a^<(0, \tau')} \right], \end{aligned} \quad (\text{D.4})$$

where we have inserted the identity operator $e^{i\sqrt{2\pi K} \phi_s^>(x', \tau')} e^{-i\sqrt{2\pi K} \phi_s^>(x', \tau')}$ in equation (D.4). The leading contribution in the bracket $[\dots]$ of equation (D.4) is given by:

$$\begin{aligned} [\dots] = & -2\pi i \partial_x \left\langle \theta_s^>(x, \tau) \phi_s^>(x', \tau') \right\rangle_f \Big|_{x, x' \rightarrow 0} \\ & \times \left\langle e^{i\sqrt{\frac{2\pi}{K}} \theta_a^>(0, \tau')} \right\rangle_f e^{i\sqrt{\frac{2\pi}{K}} \theta_a^<(0, \tau')}. \end{aligned} \quad (\text{D.5})$$

With the help of equation (A.20), carrying out the integral over the fast modes and performing rescaling, we arrive at:

$$\delta j_2^{xy} = -\frac{\pi}{v_F'} \frac{J_2^{xy} \delta J_1^z}{2\pi a} \int d\tau S^+ \left(\frac{\mu'}{\mu} \right)^{\frac{1}{k}-1+\frac{1}{2k}} \frac{d\mu}{\mu} \times F_s \left[F_f e^{i\theta_a^<(0,\tau)} + F_f^\dagger e^{-i\theta_a^<(0,\tau)} \right], \quad (D.6)$$

where the scaling dimension for S_z : $[S_z] = \frac{1}{2k}$ is used. Therefore, we have reproduced the RG scaling equation for j_2^{xy} at the 2CK fixed point in equation (19) with the proper definitions for the renormalized Kondo couplings: $j_2^{xy} \equiv \rho_0 \mu^{\frac{1}{k}-1} J_2^{xy}$, $\delta j_1^z \equiv \frac{\rho_0}{v_F'} \mu^{\frac{1}{2k}} \delta J_1^z$.

Next, we compute the renormalization of δj_1^z contributed from the $(J_2^{xy})^2$ term:

$$\delta j_1^z = \left(\frac{J_2^{xy}}{2\pi a} \right)^2 F_s F_f F_s^\dagger F_f^\dagger \times \int d\tau \int d\tau' S^+(\tau) S^-(\tau') \left[\left\langle e^{i\sqrt{\frac{2\pi}{K}} \theta_a(0,\tau)} e^{-i\sqrt{\frac{2\pi}{K}} \theta_a(0,\tau')} \right\rangle_f - \left\langle e^{i\sqrt{\frac{2\pi}{K}} \theta_a(0,\tau)} \right\rangle_f \left\langle e^{-i\sqrt{\frac{2\pi}{K}} \theta_a(0,\tau')} \right\rangle_f \right] \quad (D.7)$$

Carrying out averaging over the fast modes, we have:

$$\delta j_1^z = -\left(\frac{J_2^{xy}}{2\pi a} \right)^2 \times \int d\tau \int d\tau' S_z(\tau) \left(\frac{\mu'}{\mu} \right)^{2\left(\frac{1}{k}-1\right)} \times \left[\left(\frac{\mu'}{\mu} \right)^{\frac{1}{k}-1} - 1 \right] e^{i\sqrt{\frac{2\pi}{K}} \theta_a^<(0,\tau)} e^{-i\sqrt{\frac{2\pi}{K}} \theta_a^<(0,\tau')} \quad (D.8)$$

Upon Taylor expanding the exponential $e^{i\sqrt{\frac{2\pi}{K}} \theta_a^<(0,\tau)}$, we arrive at:

$$e^{i\sqrt{\frac{2\pi}{K}} \theta_a^<(0,\tau)} e^{-i\sqrt{\frac{2\pi}{K}} \theta_a^<(0,\tau')} \approx 1 + i\sqrt{\frac{2\pi}{K}} \left[\theta_a^<(0,\tau) - \theta^<(0,\tau') \right] \quad (D.9)$$

Near the 2CK fixed point, the term $\theta_a^<(0,\tau) - \theta^<(0,\tau')$ can be re-expressed via the open boundary conditions at 2CK in the limit of $x \approx a \rightarrow 0$ with a being the lattice constant as:

$$\theta_i(x,\tau) = \phi_{iL}(x,\tau) - \phi_{iR}(x,\tau) = \phi_{iL}(x,\tau) + \phi_{iL}(-x,\tau) \approx 2\phi_{iL}(0,\tau) + x^2 \left[\partial_x^2 \phi_{iL}(x,\tau) \Big|_{x \rightarrow 0} \right] + \mathcal{O}(x^3), \quad (D.10)$$

and

$$\theta_a(x,\tau) = \theta_a(0,\tau) + \frac{x^2}{2} \left[\partial_x^2 (\phi_{1L}(x,\tau) + \phi_{2R}(x,\tau)) \Big|_{x \rightarrow 0} \right] + \mathcal{O}(x^3), \\ -\theta_a(x,\tau') = -\theta_a(0,\tau') + \frac{x^2}{2} \left[\partial_x^2 (\phi_{1R}(x,\tau') + \phi_{2L}(x,\tau')) \Big|_{x \rightarrow 0} \right] + \mathcal{O}(x^3), \quad (D.11)$$

where we have used the 2CK boundary condition: $\phi_i^L(x) = -\phi_i^R(-x)$, and we ignore here the higher order terms $\mathcal{O}(x^3)$ and beyond. In the limit of $\tau \rightarrow \tau'$, we have, therefore

$$\int d\tau \int d\tau' \left[\theta_a(0,\tau) - \theta_a(0,\tau') \right] = \int d\tau \int d\tau' \left[\theta_a(x,\tau) - \theta_a(x,\tau') - \frac{x^2}{2} \left(\partial_x^2 \phi_s(x,\tau) \Big|_{x \rightarrow 0} \right) + \mathcal{O}(x^3) \right] \approx \int d\tau \int d\tau' \left[\tau \partial_\tau \theta_a(x,\tau) - \frac{a^2}{2} \partial_x^2 \phi_s(x,\tau) \Big|_{x \rightarrow 0} \right] \quad (D.12)$$

With the help of the identity equation (A.20), equation (D.12) can be re-written as:

$$\int d\tau \int d\tau' S_z(\tau) \left[\theta_a(0,\tau) - \theta_a(0,\tau') \right] \approx i \int d\tau S_z(\tau) \left[v_F' \tau_0 \partial_x \phi_a(x,\tau) + \frac{a^2}{2} \frac{1}{v_F'} \partial_x \theta_s(0,\tau) \right]. \quad (D.13)$$

The first term in equation (D.13) can be simplified in the limit of $x \approx a \rightarrow 0$ as:

$$\begin{aligned} & i v_F' \tau_0 \int d\tau S_z(\tau) \partial_x \phi_a(x=a, \tau) \\ & \approx i v_F' \tau_0 \int d\tau S_z(\tau) \left[\partial_x \phi_a(0, \tau) + a \partial_x^2 \phi_a(0, \tau) \right] \end{aligned} \quad (\text{D.14})$$

where $\partial_x \phi_a(0, \tau) \propto \rho_1(0, \tau) - \rho_2(0, \tau) = 0$ with $\rho_i(0, \tau)$ being the charge density of the lead i at $x=0$, which vanishes for $x=0$ ($\rho_i(0, \tau) = 0$) due to the open boundary condition at the 2CK fixed point (the electron wave function and therefore its charge density vanishes at $x=0$). Therefore, the remaining part in equation (D.14) becomes

$$i v_F' \tau_0 \int d\tau \tilde{\mathcal{A}}(\tau) \quad (\text{D.15})$$

where the operator $\tilde{\mathcal{A}}(\tau)$ is defined as:

$$\tilde{\mathcal{A}}(\tau) = S_z(\tau) \partial_x^2 \phi_a(0, \tau). \quad (\text{D.16})$$

It is straightforward to see that $\tilde{\mathcal{A}}$ is a highly irrelevant operator with a scaling dimension $[\tilde{\mathcal{A}}] = 2 + \frac{1}{2K} > 1$ for any $K > 0$; we therefore ignore it here.

The second term in equation (D.13) (proportional to $\partial_x \theta_s(0, \tau)$) will contribute to the renormalization of the \tilde{j}_1^z term. Combining everything from equation (D.7) to equation (D.16), the one-loop RG scaling equation for δj_1^z becomes:

$$\frac{d\delta j_1^z}{d \ln \mu} = e' \delta j_1^z - \frac{(J_2^{xy})^2}{8\pi v_F'}. \quad (\text{D.17})$$

With the proper rescaling of J_2^{xy} : $J_2^{xy} \rightarrow \frac{1}{\sqrt{8\pi v_F'}} J_2^{xy}$, we finally reproduce the RG scaling equation for \tilde{j}_1^z in equation (19).

In fact, the above results can be understood alternatively in terms of non-vanishing correlator $\langle \hat{\mathcal{O}} \rangle \equiv \langle \hat{j}_2^{xy}(0, \tau) \hat{j}_2^{xy}(0, \tau') \hat{\delta}_1^z(x, \bar{\tau}) \rangle$, which measures the cross-correlations between the δj_1^z and \tilde{j}_2^{xy} terms at the 2CK fixed point under one-loop RG. Here, $\hat{\delta}_1^z, \hat{j}_2^{xy}$ refer to the bosonic operators associated with the δj_1^z and \tilde{j}_2^{xy} terms, respectively. A typical term in $\hat{\mathcal{O}}$ reads:

$$\langle \hat{\mathcal{O}} \rangle \sim \left\langle e^{i\theta_a(0, \tau)} e^{-i\theta_a(0, \tau')} \partial_x \theta_s(x \rightarrow 0, \bar{\tau}) \right\rangle. \quad (\text{D.18})$$

Via equation (D.12) and the 2CK open boundary condition, in the limit of $x, \tau \rightarrow 0$ and $\tau' = 0$, we have

$$\begin{aligned} \theta_a(0, \tau) - \theta_a(0, \tau') & \approx \theta_a(x, \tau) - \theta_a(x, \tau') \\ & - \frac{x^2}{2} \left[\partial_x^2 (\phi_1^R(x, \tau) + \phi_2^L(x, \tau) \right. \\ & \left. + \phi_1^L(x, \tau) + \phi_2^R(x, \tau)) \Big|_{x \rightarrow 0} \right] + \dots \\ & = \tau \partial_\tau \theta_a(x, \tau) - \frac{a^2}{2} \partial_x^2 \phi_s(x, \tau) \Big|_{x \rightarrow 0} + \dots \end{aligned} \quad (\text{D.19})$$

where \dots refers to the higher order contributions. Note that the term $a^2 \partial_x^2 \phi_s(x, \tau) \Big|_{x \rightarrow 0}$ in equation (D.19) is related to $\partial_x \theta_s(0, \tau)$ via equation (A.20):

$$\frac{a^2}{2} \partial_x^2 \phi_s(x, \tau) \Big|_{x \rightarrow 0} = \frac{ia^2}{v_F'} \partial_\tau \partial_x \theta_s(0, \tau). \quad (\text{D.20})$$

With the above relations, equation (D.18) becomes:

$$\begin{aligned} \langle \hat{\mathcal{O}} \rangle & \sim \left\langle e^{-\frac{a^2}{2v_F'} \partial_\tau \partial_x \theta_s(0, \tau)} \partial_x \theta_s(0, \bar{\tau}) \right\rangle \\ & \approx \left\langle \left(1 - \frac{a^2}{2v_F'} \partial_\tau \partial_x \theta_s(0, \tau) \right) \partial_x \theta_s(0, \bar{\tau}) \right\rangle \\ & = -\frac{a^2}{2v_F'} \partial_\tau \left\langle \partial_x \theta_s(0, \tau) \partial_x \theta_s(0, \bar{\tau}) \right\rangle \end{aligned} \quad (\text{D.21})$$

where we have dropped the term $\tau \partial_x \theta_a(x, \tau) = \frac{i\tau}{v_F} \partial_x \phi_a(x, \tau)$ in equation (D.19) as $\langle \partial_x \phi_a(x, \tau) \partial_x \theta_s(x, \tau) \rangle$ vanishes. It is clear from equation (D.21) that the correlator gets a finite expectation value as $\langle \partial_x \theta_s(0, \tau) \partial_x \theta_s(0, \bar{\tau}) \rangle$ does not vanish:

$$\left\langle \partial_x \theta_s(0, \tau) \partial_x \theta_s(0, \bar{\tau}) \right\rangle = \lim_{\eta \rightarrow 0} \frac{1}{\eta^2} \partial_x \partial_{\bar{x}} \left\langle e^{i\eta \theta_s(x, \tau)} e^{-i\eta \theta_s(\bar{x}, \bar{\tau})} \right\rangle \neq 0 \quad (\text{D.22})$$

as the correlator $\langle \theta_s(x, \tau) \theta_s(\bar{x}, \bar{\tau}) \rangle$ is a non-trivial function of $x - \bar{x}$ and $\tau - \bar{\tau}$.

Note that although $\theta_a(0, \tau)$ decouples from $\theta_s(0, \tau)$, due to the 2CK open boundary condition, the correlator $\langle \hat{j}_2^{xy}(0, \tau) \hat{j}_2^{xy}(0, \tau') \hat{j}_1^z(0, \bar{\tau}) \rangle$ does not vanish. This alternative route provides us with a justification of our previous derivations for the RG scaling equations equation (19) via re-fermionization.

References

- [1] Sachdev S 2000 *Quantum Phase Transitions* (Cambridge: Cambridge University press)
- [2] Sondhi S L, Girvin S M, Carini J P and Shahar D 1987 *Rev. Mod. Phys.* **69** 315
- [3] Kouwenhoven L and Glazman L 2001 *Phys. World* **14** 33
- [4] Goldhaber-Gordon D *et al* 1998 *Nature* **391** 156
- [5] van der Wiel W G *et al* 2000 *Science* **289** 2105
- [6] Glazman L I and Raikh M E 1988 *Sov. Phys. JETP Lett.* **47** 452
- [7] Ng T K and Lee P A 1988 *Phys. Rev. Lett.* **61** 1768
- [8] le Hur K 2004 *Phys. Rev. Lett.* **92** 196804
- [9] Li M-R, le Hur K and Hofstetter W 2005 *Phys. Rev. Lett.* **95** 086406
- [10] le Hur K and Li M 2005 *Phys. Rev. B* **72** 073305
- [11] Furusaki A and Matveev K A 2002 *Phys. Rev. Lett.* **88** 226404
- [12] Vojta M 2006 *Phil. Mag.* **86** 1807
- [13] Zarand G, Chung C-H, Simon P and Vojta M 2006 *Phys. Rev. Lett.* **97** 166802
- [14] Chung C H and Hofstetter W 2007 *Phys. Rev. B* **76** 045329
- [15] Chung C-H, Glossop M T, Fritz L, Kircan M, Ingersent K and Vojta M 2007 *Phys. Rev. B* **76** 235103
- [16] Chung C-H, Zarand G and Wölfle P 2008 *Phys. Rev. B* **77** 035120
- [17] Hofstetter W and Shoeller H 2002 *Phys. Rev. Lett.* **88** 016803
- [18] Vojta M, Bulla R and Hofstetter W 2002 *Phys. Rev. B* **65** 140405
- [19] Sela E and Affleck I 2009 *Phys. Rev. Lett.* **102** 047201
- [20] Chung C-H, le Hur K, Vojta M and Wölfle P 2009 *Phys. Rev. Lett.* **102** 216803
- [21] Chung C-H, Latha K V P, le Hur K, Vojta M and Wölfle P 2010 *Phys. Rev. B* **82** 115325
- [22] Kirchner S and Si Q 2009 *Phys. Rev. Lett.* **103** 206401
- [23] Mitra A and Rosch A 2011 *Phys. Rev. Lett.* **106** 106402
- [24] Hewson A C 1997 *Kondo Problems to Heavy Fermions* (Cambridge: Cambridge University Press)
- [25] Goldhaber-Gordon D, Shtrikman H, Mahalu D, Abusch-Magder D, Meirav U and Kastner M A 1998 *Nature* **391** 156
- [26] van der Wiel W G, de Franceschi S, Fujisawa T, Elzerman J M, Tarucha S and Kouwenhoven L P 2000 *Science* **289** 2105
- [27] Kouwenhoven L and Glazman L 2001 *Phys. World* **14** 33
- [28] Cox D L and Zawadowski A 1998 *Adv. Phys.* **47** 599
- [29] Nozière P and Blandin A 1980 *J. Phys.* **41** 193
- [30] Affleck I and Ludwig A W W 1990 *Nucl. Phys. B* **360** 641
- [31] Affleck I and Ludwig A W W 1991 *Phys. Rev. Lett.* **67** 161
- [32] Fendley P, Lesage F and Saleur H 1995 *J. Stat. Phys.* **79** 799
- [33] Hettler M H, Kroha J and Hershfield S 1994 *Phys. Rev. Lett.* **73** 1968
- [34] Hettler M H, Kroha J and Hershfield S 1998 *Phys. Rev. B* **58** 5649
- [35] Fendley P, Fisher M P A and Nayak C 2007 *Phys. Rev. B* **75** 045317
- [36] Fiete G A, Bishara W and Nayak C 2008 *Phys. Rev. Lett.* **101** 176801
- [37] Sela E, Mitchell A K and Fritz L 2011 *Phys. Rev. Lett.* **106** 147202
- [38] Mitchell A K, Sela E and Logan D E 2012 *Phys. Rev. Lett.* **108** 086405
- [39] Potok R M, Rau I G, Shtrikman H, Oreg Y and Goldhaber-Gordon D 2007 *Nature* **446** 167
- [40] Yeh S S and Lin J J 2009 *Phys. Rev. B* **79** 012411
- [41] Ralph D C and Buhrman R A 1992 *Phys. Rev. Lett.* **69** 2118
- [42] Fabrizio M and Gogolin A O 1995 *Phys. Rev. B* **51** 17827
- [43] Rincon J, Garcia D J, Hallberg K and Vojta M 2013 *Phys. Rev. B* **88** 140407 (R)
- [44] Kim E arXiv:condmat/0106575 (unpublished)
- [45] Kane C L and Mele E J 2005 *Phys. Rev. Lett.* **95** 226801
- [46] Bernevig B A, Hughes T A and Zhang S C 2006 *Science* **314** 1757
- [47] Fu L, Kane C L and Mele E J 2007 *Phys. Rev. Lett.* **98** 106803
- [48] König M, Wiedmann S, Brune C, Roth A, Buhmann H, Molenkamp L W, Qi X-L and Zhang S-C 2007 *Science* **318** 766
- [49] Hsieh D, Qian D, Wray L, Xia Y, Hor Y S, Cava R J and Hasan M Z 2008 *Nature* **452** 970
- [50] Hsieh D *et al* 2009 *Science* **323** 919–22
- [51] Hasan M Z and Kane C L 2010 *Rev. Mod. Phys.* **82** 3045
- [52] Wu C, Bernevig B A and Zhang S C 2006 *Phys. Rev. Lett.* **96** 106401
- [53] Law K T, Sheng C Y, Lee P A and Ng T K 2010 *Phys. Rev. B* **81** 041305(R)
- [54] Zawadowski A and Fazekas P 1969 *Physik Z* **226** 235
- [55] Coleman P 1984 *Phys. Rev. B* **29** 3035
- [56] Costi T A, Kroha J and Wölfle P 1996 *Phys. Rev. B* **53** 1850

- [31] Gogolin A O, Nersisyan A A and Tsvelik A M 1998 *Bosonization and Strongly Correlated Systems* (Cambridge: Cambridge University Press)
Giamarchi T 2004 *Quantum Physics in One Dimension* (Oxford: Oxford University Press)
Delft J V and Schoeller H 1998 *Ann. Phys.* **7** 225
- [32] Teo Jeffrey C Y and Kane C L 2009 *Phys. Rev. B* **79** 235321
- [33] Kim M D, Kim C K, Nahm K and Ryu C-M 2001 *J. Phys.: Condens. Matter* **13** 3271
- [34] Florens S, Simon P, Andergassen S and Feinberg D 2007 *Phys. Rev. B* **75** 155321
- [35] Emery V J and Kivelson S 1992 *Phys. Rev. B* **46** 10812
- [36] Kane C L and Fisher M P A 1992 *Phys. Rev. Lett.* **68** 1220
- [37] Brezin E, Le Guillou J C and Zinn-Justin J 1996 *Phase Transitions and Critical Phenomena* vol 6 ed C Domb and M S Green (Norwich: Page Bros)
Zinn-Justin J 2002 *Quantum Field Theory and Critical Phenomena* (Oxford: Clarendon Press)
- [38] Zarand G and Demler E 2002 *Phys. Rev. B* **66** 024427
- [39] Zhu L and Si Q 2002 *Phys. Rev. B* **66** 024426
- [40] Kircan M and Vojta M 2004 *Phys. Rev. B* **69** 174421
- [41] Fritz L and Vojta M 2004 *Phys. Rev. B* **70** 214427
- [42] Paaske J, Rosch A, Kroha J and Wölfle P 2004 *Phys. Rev. B* **70** 155301
- [43] Ingersent K and Si Q M 2002 *Phys. Rev. Lett.* **89** 076403
Vojta M 2006 *Phil. Mag.* **86** 1807
- [44] Fabrizio M and Gogolin A O 1994 *Phys. Rev. B* **50** 17732
- [45] Fritz L, Florens S and Vojta M 2006 *Phys. Rev. B* **74** 144410

Copyright of New Journal of Physics is the property of IOP Publishing and its content may not be copied or emailed to multiple sites or posted to a listserv without the copyright holder's express written permission. However, users may print, download, or email articles for individual use.